NON-STATIONARY MODELING OF ROAD-CURVE CRASH FREQUENCY WITH GEOGRAPHICALLY WEIGHTED REGRESSION

by

Ce Wang

A Thesis

Submitted to the Faculty of Purdue University

In Partial Fulfillment of the Requirements for the degree of

Master of Science in Civil Engineering

Lyles School of Civil Engineering

West Lafayette, Indiana

May 2021

THE PURDUE UNIVERSITY GRADUATE SCHOOL
STATEMENT OF COMMITTEE APPROVAL

Dr. Jie Shan, Chair

Lyles School of Civil Engineering

Dr. Konstantina Gkritza

Lyles School of Civil Engineering

Dr. Shuo Li

Division of Research and Development
Indiana Department of Transportation

Approved by:

Dr. Dulcy Abraham

ACKNOWLEDGMENTS

First and foremost, I am sincerely grateful to my advisor, Dr. Jie Shan, for his continuous and enthusiastic support of my research as well as for giving me the opportunity for a research assistantship. The work experience I have gained and the skills I have developed during my time at Purdue are invaluable. I am also thankful to the other members of my advisory committee, Dr. Konstantina Gkritza and Dr. Shuo Li, for their kindness, encouragement, and insightful comments.

I am additionally grateful to Dr. Shuo Li for granting me access to the resources and the valuable datasets of Indiana Department of Transportation Research and Development for my research. This unique exposure helped me develop skills that will serve me well as I go forward in my career.

I am extremely grateful as well to the following individuals who shared their knowledge with me: Yunchang Zhang, who unreservedly offered me instructive advice on my research; Zhixin Li, who helped me with basic geomatics theory and coding skills; Xiaoyi Peng, who was a research team member with me through thick and thin; Joseph Grocholski, who helped me with thesis writing corrections; and Xiangxi Tian, who gave me thesis advice. I am also thankful to Indiana Map and FHWA for the open access I received to the data used in my research.

Last but not the least, I am eternally grateful to my parents for supporting me both financially and spiritually throughout my entire graduate studies and for their unceasing encouragement and support.

TABLE OF CONTENTS

LIST OF TABLES

LIST OF FIGURES

LIST OF ABBREVIATIONS

AADT	Annual Average Daily Traffic
AICc	Corrected Akaike Information Criterion
CMF	Crash Modification Factors
EB	Empirical Bayes
FHWA	Federal Highway Administration
GWNBR	Geographically Weighted Negative Binomial Regression
GWNBRg	Geographically Weighted Negative Binomial Regression with global dispersion parameter
GWPR	Geographically Weighted Poisson Regression
GWR	Geographically Weighted Regression
HFST	High Friction Surface Treatment
INDOT	Indiana Department of Transportation
MAD	Median Absolute Deviation
NB	Negative Binomial
ROCA	Road Curvature Analyst
RPNB	Random Parameter Negative Binomial
SPF	Safety Performance Function
TAZ	Traffic Analysis Zone
VMT	Vehicle Miles Traveled
ZINB	Zero-inflated Negative Binomial

ABSTRACT

Vehicle crashes on roads are caused by many factors. However, the influence of these factors is not necessarily homogenous across locations, which is a challenge for non-stationary modeling approaches. To address this problem, this thesis not only evaluated the safety performance of high friction surface treatment (HFST) installations throughout Indiana using empirical Bayes (EB) analysis, but also adopted two types of methods that allowed the parameters to fluctuate among observations (the random parameter approach and the geographically weighted regression or GWR approach). With road curvature, curve length, pavement friction, and traffic volume as the independent variables, this thesis modeled vehicle crash frequencies using two non-spatial models (the negative binomial (NB) model and the random parameter negative binomial (RPNB)), as well as three spatial models (the GWR approach including geographically weighted Poisson regression (GWPR), the geographically weighted negative binomial regression (GWNBR), and the global geographically weighted negative binomial regression (GWNBRg). These models then were calibrated at the macro-level and micro-level using a dataset of 9,415 horizontal curve segments with a total length of 1,545 kilometers for a period of three years (2016-2018) throughout Indiana. The results revealed that the GWR approach successfully captured spatial heterogeneity and thereby significantly outperformed the conventional non-spatial approach. Among the GWR models, the GWNBR model performed better for the Akaike Information Criterion (AICc) and the spatial distribution of the coefficients. This thesis also found that pavement friction and curve length had less influence on crash frequency in forest areas than in plain areas. Furthermore, pavement friction tended to have the most considerable impact on crash frequency in unpopulated areas with sparse curve distributions. It is expected the findings of the thesis can be used for Indiana highway curve safety improvement and other transportation applications that need to consider spatial heterogeneity.

1. INTRODUCTION

1.1 Background

Road horizontal curve is a known critical factor for vehicle crashes due to its disproportionate number of crashes compared to other geometric features. Traffic crashes cost over 30,000 lives in America every year. According to the U.S. Federal Highway Administration (FHWA), more than 25% of those fatal crashes are related to horizontal curves, which occur on only 10% of the total system of mileage (FHWA 2011).

To explore the intrinsic law of this phenomenon, several prediction models have been developed for curve crashes over the past decades. In terms of pavement condition, Buddhavarapu et al. (2013) developed a crash injury severity model on two-lane horizontal curves in Texas and found that curve segments with smoother pavements appeared to be more likely to be high-risk while longitudinal skid measurements showed little correlation with curve crash injury severity. To explore the influence of geometric features on curve crash frequency, an NB model was developed by Schneider et al. (2010) for single-vehicle motorcycle crashes that occurred on curve segments of rural two-lane highways in Ohio. The authors determined that the geometric feature variables that significantly influenced motorcycle crash frequency were the curve radius, curve length, and curve shoulder width. Moreover, Musey and Park (2016) proposed a model for predicting horizontal curve crash severity using pavement friction and road curvature. Their results revealed that serious injuries occurred on curves with a higher degree of curvature and that lower friction was closely correlated to wet pavement crashes. Meanwhile, Gooch et al. (2016) found that the correlation of crash frequency at adjacent curves was significant.

All the aforementioned models were global, i.e., they assumed that the parameter estimates were fixed across the geographical region of analysis. However, in reality, as location information is collected for reference to crash data, some of the predicting variables may not be stationary. For example, the geometry features (e.g., radius and length) of horizontal curves may cause observation heterogeneity from unobserved factors such as various driver responses on curves, time-varying traffic, and weather conditions (Venkataraman et al. 2014). The effects of pavement friction also may vary across observations due to friction variations, heterogeneous driver behavior responses, and climate influences. In terms of the effect of traffic volume on crash likelihood,

heterogeneous driver reactions to traffic may exist as well as environmental factors (Mannering et al. 2016). Hence, modeling the relation between crash count and such explanatory variables with overall fixed coefficients for the entire study area could cause biased estimates of the individual parameters. Thus, adding spatial variance to non-stationary models, such as geographically weighted regression (GWR) and random parameter approaches, may provide a better view for developing spatial dependency over space.

Traffic safety spatial studies are categorized as two levels of spatial aggregation: macro-level and micro-level. Conventionally, micro-level analysis focuses on specific road entities of the road network, such as intersections, railways, corridors, and road segments (Cai et al. 2018, Schneider IV et al. 2010; Wan 2018). However, macro-level analysis, which focuses on zonal level crashes with various spatial units, is becoming popular as part of the transportation planning process in research studies. The spatial units that have been comprehensively developed recently include traffic analysis zones (TAZs) (Duddu and Pulugurtha 2012; Lee et al. 2014; Gomes et al. 2017; Soroori et al. 2020); counties (Aguero-Valverde and Jovanis 2006; Huang et al. 2010); census tracts (Abdel-Aty et al. 2013); wards (Quddus 2008; Wang et al. 2009); and statistical area levels (Amoh-Gyimah et al. 2016a). One of the advantages associated with macro-level crash modeling is that it does not count on detailed data as much as micro-level crash models (Amoh-Gyimah et al. 2017). However, it has been proven that micro-level models with less detailed data still provide an acceptable accuracy when applied to non-stationary models (Anastasopoulos and Mannering 2011). It is reasonable and promising, therefore, to employ non-stationary models (i.e., GWR and random parameter) for micro-level safety analysis.

As previously stated, the additional centripetal force that is exerted on vehicles by friction and radius is one of the most important reasons for the vulnerability of highway curves for crash occurrence. One of the current popular methods for improving the friction of pavement in the U.S. is to apply a high friction surface treatment (HFST), which consists of a high-quality and durable aggregate on top of a resin binder to help prevent drivers from losing control of their vehicles. The most promising proven effect of HFST has been a significant reduction in crashes, injuries, and ultimately fatalities in wet weather and high-speed situations. Hence, HFST has been proactively promoted by FHWA as a cost-effective solution to pavement friction-related vehicle crashes, including run-off-road, tailgating, and head-on crashes, particularly on two-lane roads or at intersections and under wet pavement conditions. Figure 1.1 shows the status of HFST

implementation on curves in the U.S. as of December 2018 (FHWA 2021). To further improve traffic safety, the Indiana Department of Transportation (INDOT) launched an initiative to carry out HFST projects with a total value of more than $1 million in the state of Indiana at designated potentially high-crash areas in 2018.

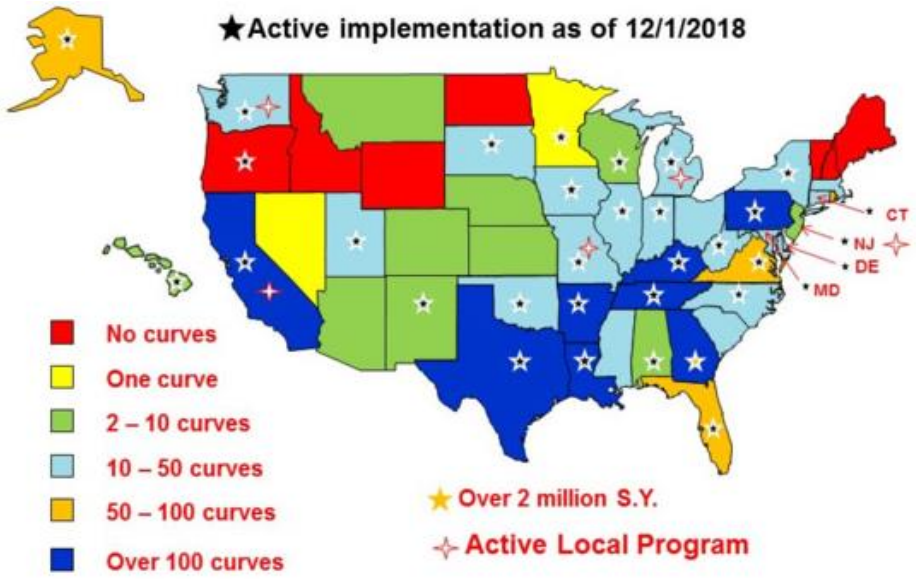

Figure 1.1. Locations of Major HFST Installations in the U.S. (FHWA 2018).

1.2 Objectives

This thesis aimed to conduct a comprehensive review and analysis of the relationship of highway curve crash frequency and curve segment features as a proof of concept in order to further explore the safety performance of HFST in Indiana. The objectives of this thesis were as follows.

- Perform a before-after analysis of HFST installations.
- Develop statewide highway curve crash frequency models along with exposure parameters, pavement friction, and radius from macro-level and micro-level datasets.
- Compare the performance of conventional stationary and non-stationary models in terms of goodness of fit.
- Explore the capability of capturing the spatial heterogeneity occurring in the relationship of the GWR approaches and further discuss local patterns presented.

With respect to the HFST safety performance evaluation, conventional before-after comparisons always have a “regression-to-the-mean” problem. This thesis applied empirical

Bayes (EB) analysis to provide a reliable Indiana HFST safety assessment. To offer a different view of the selection of the construction location, this thesis further modeled the statewide INDOT highway curve crash data provided. Considering the fact that previous research studies were mostly conducted at the macro-level (zonal level) or the micro-level (each observation), this research explored different strategies for modeling local variations of over-dispersed crash count data in statewide highway horizontal curves in relation to the curve segment characteristics at both levels. From the results of nonstationary modeling, the local pattern of the variables' relationships and spatial heterogeneity can display factors that influence variance over space, which needs further investigation.

1.3 Previous work

Since the first installations of HFST in the U.S. in the early 2000s, scholars and state departments of transportation (DOTs) have continued to explore its safety performance. As HFST is a relatively high-cost treatment and currently has limited applications, i.e., ramps and curves, evaluating its safety performance is not yet precise. The performance of safety improvement countermeasures is always presented by crash modification factors (CMFs), the theory of which is introduced in Chapter 2. Recently, Wilson et al. (2016) conducted a naïve before-after comparison in Florida and concluded that HFST only showed superior crash reduction on tight curves and wet weather crash occurrence. However, Merritt et al. (2015) and Lyon et al. (2020) insisted that a regression-to-the-mean problem should not be neglected and suggested that EB analysis is the best option.

Compared to other states that implemented HFST, Indiana has much less experience both conducting and evaluating their program. Retrospective research conducted by other states provide a reference and big picture of HFST's effect on crash reduction. Kentucky was one of the earliest states to install HFST and several studies observed a significant reduction in crash occurrence with HFST. Albin et al. (2016) observed a crash reduction of about 70% on 30 curves since 2009; Von Quintus & Mergenmeier (2015) found that crashes declined about 73% since 43 HFST projects between 2009 and 2012. California has implemented over 100 HFST projects since 2011, and Peterson et al. (2016) found an over 50% annual crash reduction. In Pennsylvania, HFST has been installed since 2007; and Musey (2017) did a thorough safety evaluation on 68 statewide sites and observed a CMF of 0.67.

Observations with too many zero counts present a challenging research problem of great importance. Miaou (1994) and Shankar et al. (1997) developed and applied zero-inflated methods on crash modeling, which separate models into two-state regimes, i.e., a zero-count state and a normal count state. Some recent studies developed diverse zero-inflated types of models. For example, Dong et al. (2014) studied Tennessee intersection crash frequency using a multivariate zero-inflated Poisson model and found that it could provide more accurate estimating. Kim et al. (2016) predicted traffic crashes based on the behaviors of drivers and their past violation records in Korea using a zero-inflated negative binomial model (ZINB). Liu et al. (2018) applied a multivariate random parameter ZINB that could account for excess zeros and heterogeneity on urban midblock segment crash frequency in Nebraska. Raihan et al. (2019) also investigated the relationship between bicycle rider behavior and bicycle CMFs in Florida utilizing ZINB models.

A number of road crash analysis methods have been developed to determine the spatial dependency and heterogeneity of the influence of a parameter and to pinpoint high-risk locations (Ziakopoulos and Yannis,2020). These methods included GWR (Hadayeghi 2010); Bayesian models with conditional autoregressive (Quddus 2008); autoregressive models with spatial spillover effects (Cai et al. 2016); full Bayes multiple membership spatial model (El-Basyouny and Sayed 2009); and random parameter models (Xu and Huang 2015).

However, the GWR approach is the most promising technique to reveal the variables' heterogenous effects over space in crash counts modeling (Ziakopoulos and Yannis 2020). To address the issue that some variables have more impacts in certain spatial locations but fewer impacts in others, the GWR approach was applied in this thesis. For comparison, the random parameter approach also was utilized as it also allows parameters varying from each other but no spatial relationship is involved. Since Fotheringham et al. (2002) systematically illustrated GWR theory, this technique often has been applied to road safety analysis (Hadayeghi et al. 2003). Hadayeghi et al. (2010a) explored application of the GWR approach to count data modeling for traffic safety analysis at the TAZ level. Li et al. (2013) evaluated the performance of a geographically weighted Poisson regression (GWPR) model in comparison to a traditional generalized linear model (GLM) on county level crash data. Based on the semi-parametric GWPR model study of Nakaya et al. (2005), where some variables may not significantly vary over space while others are spatially heterogeneous, Xu and Huang (2015) examined Florida macro-level crash data with a random parameter negative binomial model (RPNB) and a semi-parametric

GWPR model. Silva and Rodrigues (2014) extended the GWPR to model over-dispersed data by a geographically weighted negative binomial regression (GWNBR) model and a GWNBR model with global over-dispersion parameters (GWNBRg). Gomes et al. (2017) and Soroori et al. (2020) applied a GWNBR to model over-dispersed crashes for traffic zones, which outperformed the GWPR and traditional global models. Amoh-Gyimah et al. (2017) found that when compared with the RPNB models and a GLM model, the GWR approach provided better performance on macroscopic over-dispersed traffic crash frequency modeling. Nevertheless, only a few existing studies investigated modeling statewide micro-level regional safety on over-dispersed crash data. Statewide non-stationary crash frequency modeling involves a coefficient variance on a larger number of observations and spacious areas. Therefore, the spatial heterogeneity of larger-scale crash data using the GWR approach needs to be further investigated.

The RPNB model, which also addresses unobserved heterogeneity in regional safety over-dispersed data modeling, assumes that the parameters draw from some random distributions and vary randomly from case to case. To investigate the unobserved heterogeneity across highway segments for crash count prediction, Shaon et al. (2018a and b) and Chen et al. (2019) applied random parameter Poisson-based models in their safety studies. As a branch of random parameter Poisson-based modeling, the RPNB model has been widely used to account for data over-dispersion, including Venkataraman et al. (2011, 2013, 2014), Chen and Tarko (2014), and Saeed et al. (2019). Also, Xin et al. (2017a, b) developed an RPNB model for Florida horizontal curves along two-lane, undivided highways for motorcycle crashes with curve design factors. However, very few studies to date have focused on statewide highway curve over-dispersed crash count modeling.

1.4 Structure of the thesis

This remainder of this thesis proceeds as follows. Chapter 2 presents CMF theory and EB analysis principles and introduces the stationary and non-stationary methods that were applied to Indiana highway curve crash frequency modeling as well as the model goodness of fit and spatial autocorrelation evaluation approaches utilized. Chapter 3 provides information about Indiana's HFST installations, INDOT crash data sources, road network features, polyline geometry generator, traffic volume data, and pavement friction measurements. Chapter 4 first presents the HFST safety performance and statewide curve crash modeling results. Both the macro and micro

level models in stationary as well as nonstationary approaches are presented and compared. The traditional Poisson model and the GWPR model are applied to the macro level dataset, while the NB, ZINB, RPNB, and GWR approaches are implemented for a micro-level dataset. The predicted HFST CMFs based on these models also are compared with their real CMFs. Chapter 5 presents the major findings and suggestions of this thesis along with recommendations for possible future improvements.

2. METHODOLOGIES

2.1 HFST effect analysis

2.1.1 Crash Modification Factors

When considering the implementation of a particular countermeasure, such as HFST at a specific site, a CMF may be used to assess its expected safety impact. A CMF value greater than, less than, and equal to 1.0 indicate an increase, a decrease, and no change, respectively, in vehicle crashes that will result from the treatment (Gross et al. 2010).

Predicted CMF is generally developed from various crash reduction countermeasures studies. Highway Safety Manual (HSM) (AASHTO 2010) and CMF Clearinghouse are the two main resources of CMF estimation. Practitioners could apply the facilities parameter to find CMF from these resources to get basic understanding of expected impacts on roadway safety. There have been multiple methods to develop CMFs. Before-after with comparison group studies use an untreated comparison group of sites similar to the treated ones to account for changes in vehicle crashes unrelated to the treatment, such as crash trends over time and traffic volume. EB before-after studies more precisely estimate the number of crashes that would have occurred at a treated site in the after period if a treatment had not been implemented. The effect of the safety treatment is estimated by comparing this value to the number of actual crashes after treatment. Full Bayes studies use a reference group to estimate the expected crash frequency and its variance from a calibrated safety performance function (SPF) (AASHTO 2010).

2.1.2 Empirical Bayes method

Since HFSTs are installed at locations that may have higher risk than normal curve segments, before-after studies need to account for potential bias due to regression to the mean. One of the most popular ways to address the regression-to-the-mean problem is the EB procedure as outlined by Hauer (1997). SPFs are an integral part of the EB procedure (Srinivasan et al. 2013). The objective of the EB methodology is to more precisely estimate the number of crashes that would have occurred at an individual treated site in the after period if HFST had not been implemented. The approach to solve regression-to-the-mean is to generate the number of crashes expected in the after period if there is no treatment and compare it to the observed after-period crash count. The

parameters needed to calculate the number of crashes expected in the after period ($N_{\text{expected,T,A}}$) are:

- The observed number of crashes in the "before" period for the treatment group ($N_{\text{expected,T,B}}$).
- The observed number of crashes in the "after" period for the treatment group ($N_{\text{expected,T,A}}$).
- The predicted number of crashes (i.e., sum of the SPF estimates) in the "before" period ($N_{\text{predicted,T,B}}$).
- The predicted number of crashes (i.e., sum of the SPF estimates) in the "after" period ($N_{\text{predicted,T,A}}$).

The number of crashes predicted at the treated sites based on the sites with similar operational and geometric characteristics ($N_{\text{predicted,T,B}}$) is derived from the SPF. An SPF is a mathematical model that predicts the mean crash frequency for similar locations with the same characteristics. These characteristics typically include the traffic volume and may include other variables such as traffic control and geometric characteristics. All the HFST pavement sites are located on rural two-lane roads with HFST installed in both directions, except C-5, which consists of HFST installed only in one direction. The SPF used to estimate road segments in the base condition without horizontal curvature is:

$$N_{spf\ rs} = AADT \times L \times 365 \times 10^{-6} \times e^{-0.312} \quad (2\text{-}1)$$

where $N_{spf\ rs}$ is the predicted total crash frequency for a roadway segment in the base condition; AADT is the average annual traffic volume; and L is the length of roadway segment (miles).

The calibration factor for this SPF is the CMF for horizontal curvature:

$$CMF = \frac{(1.55 \times L_c) + \left(\frac{80.2}{R}\right) - (0.012 \times S)}{(1.55 \times L_c)} \quad (2\text{-}2)$$

where CMF is the crash modification factor for the effect of the horizontal alignment on the total crashes; L_C is the length of the horizontal curves (miles) which includes the spiral transition; R is the radius of the curvature (feet); and S is 1 if a spiral transition is present and 0 if a spiral transition is not present.

The predicted number of crashes (i.e., the sum of the SPF estimates) in the before period is calculated as:

$$N_{\text{predicted,T,B}} = N_{spf\ rs} \times CMF \quad (2\text{-}3)$$

The EB estimate of the expected number of crashes without treatment is computed as:

$$N_{\text{expected,T,B}} = w \times N_{\text{predicted,T,B}} + (1 - \text{w}) \times N_{\text{observed,T,B}} \quad (2\text{-}4)$$

where w is the SPF weight derived from the over-dispersion parameter in the SPF calibration process, but also depends on the number of years of crash data in the period before treatment. If the SPF has little over-dispersion, more weight is placed on the crashes predicted from the SPF ($N_{\text{predicted,T,B}}$) and less weight on the observed crash frequency ($N_{\text{observed,T,B}}$). However, the weight is reduced if many years of crash data are used. w is calculated as:

$$w = \frac{1}{1+kP} \quad (2\text{-}5)$$

where k is the over-dispersion parameter; and P is the sum of the predicted number of crashes in the before period.

For rural two-lane road segments, k is calculated as:

$$k = \frac{0.236}{L} \quad (2\text{-}6)$$

where k is the over-dispersion parameter; and L is the length of the roadway segment (miles).

Figure 2.1 illustrates how the SPF estimate is weighted with the observed crash count to estimate$N_{\text{expected,T,B}}$. It is shown that the EB estimate falls somewhere between the values from the two information sources ($N_{\text{observed,T,B}}$ and $N_{\text{predicted,T,B}}$). The regression-to-the-mean effect is the difference between $N_{\text{observed,T,B}}$ and N $N_{\text{expected,T,B}}$. Then, it is easy to get the number of crashes expected in the after period ($N_{\text{expected,T,A}}$):

$$N_{\text{expected,T,A}} = N_{\text{expected,T,B}} \times \frac{N_{\text{predicted,T,A}}}{N_{\text{predicted,T,B}}} \quad (2\text{-}7)$$

The variance of $N_{\text{expected,T,A}}$ is estimated from $N_{\text{expected,T,A}}$, the before and after SPF estimates, and the SPF weight. It is calculated as follows:

$$Var\left(N_{expected,T,A}\right) = N_{ecpected,T,A}\left(\frac{N_{predicted,T,A}}{N_{predicted,T,B}}\right)(1 - w) \quad (2\text{-}8)$$

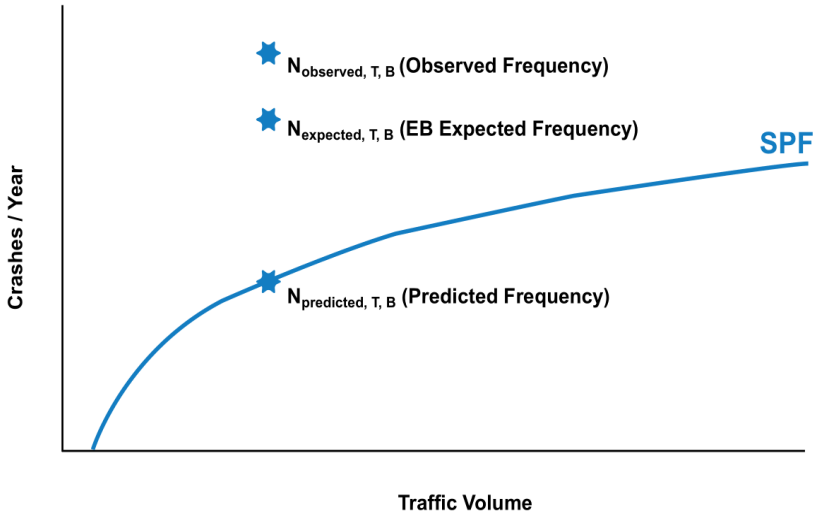

Figure 2.1. Illustration of regression-to-the-mean and EB estimate (Gross et al. 2010).

The CMF of the HFST sites is calculated as:

$$CMF = \frac{N_{\text{observed,T,A}}/N_{\text{expected,T,A}}}{1+Var(N_{\text{expected,T,A}})/N^2_{\text{expected,T,A}}} \tag{2-9}$$

The variance of the CMF is calculated as:

$$Variance\ of\ CMF = \frac{(1/N_{\text{observed,T,A}})+Var(N_{\text{expected,T,A}})/N^2_{\text{expected,T,A}}}{1+Var(N_{\text{expected,T,A}})/N^2_{\text{expected,T,A}}} \times CMF^2 \tag{2-10}$$

2.2 Stationary models

2.2.1 Negative binomial model

For non-negative integer crash count data, Poisson regression is the most basic starting point (Mannering and Bhat 2014). In the basic Poisson model, the probability of a spatial unit (curve segment) i having n_i number of crashes is given by:

$$ln(\lambda_i) = \beta_0 + \sum_{k=1}^{p} \beta_k X_{ik} \tag{2-11}$$

where λ_i is the expected number of crashes in spatial unit i, $\beta_0, \beta_1, \ldots, \beta_k$ are the model parameters, X_{ik} is the kth explanatory variable for spatial unit i. The most basic assumption to apply a Poisson model is that the dependent variable has an equal value of variance and mean (Agresti 2015). However, this assumption is often violated in crash count data. An NB regression model is generally applied to account for the issue of over-dispersion. To estimate the NB regression model,

the Poisson parameter, λ_i is specified as a function of the explanatory variables plus a gamma-distributed error term. Using a log-linear function, the NB regression model is specified as:

$$ln(\lambda_i) = \beta_0 + \sum_{k=1}^{p} \beta_k X_{ik} + \theta_i \quad (2\text{-}12)$$

Where e^{θ_i} is a gamma-distributed error term with mean 1 and variance α, and the other terms are the same as the Poisson model expression. The addition of the gamma-distributed error term allows the variance to differ from the mean such that $\text{var}(n_i) = \lambda_i + \alpha\lambda_i^2$. When α approaches zero, the NB regression is the same as with Poisson regression. The NB regression model is appropriate when α significantly differs from zero (Washington et al. 2020).

2.2.2 Zero-inflated negative binomial model

When it comes to the situation that the number of zero count observations cannot be neglected in a database, it may be attributed to two different conditions during a given time period. The first condition can arise from no events occurring during the observed period merely due to the statistical possibility of event occurrence. The other condition could result from the qualitative inability of suffering any events for certain samples, which is the "excessive" or "inflated" zero situation. Hence, the zero-inflated model came along and was applied to transportation, which separates models into two-state regimes, a zero-count state and a normal count state (Miaou 1994; Shankar et al. 1997). The ZINB model can be specified as two components:

$$\begin{aligned} count\ state: \lambda_i &= exp\left(\beta_0 + \sum_{k=1}^{p} \beta_k X_{ik} + \theta_i\right) \\ zero\ state: p_i &= \frac{exp(\gamma_0 + \sum_{k=1}^{p} \gamma_k X_{ik})}{1 + exp(\gamma_0 + \sum_{k=1}^{p} \gamma_k X_{ik})} \end{aligned} \quad (2\text{-}13)$$

where θ_i equals to 0 in a zero-inflated Poisson (ZIP) model, λ_i is the expected value of the count model for spatial unit i in the normal count state, and p_i is the possibility of an observation being qualitatively classified as the zero state $\gamma_0, \gamma_1, \ldots, \gamma_k$ are the zero model parameters.

However, to test the appropriateness of the model splitting process rather than a traditional model, the Vuong test is commonly applied (Vuong 1989). According to Vuong's statistics for traditional and zero-inflated models, if the z value is greater than 1.96, there is 95% confidence level that the statistics favor the zero-inflated model.

2.3 Non-stationary models

2.3.1 Random parameter negative binomial model

An NB model can depict the over-dispersion characteristic of traffic crash data; however, possible spatial dependency among the curve segments may be ignored, as stated previously. By incorporating a random term into the NB function, a RPNB model can be employed in response to the non-stational explanatory variables in the count models. The model is presented below:

$$\begin{gathered} ln(\lambda_i) = \beta_{i0} + \sum_{k=1}^{p} \beta_{ik} X_{ik} + \theta_i \\ \beta_{ik} = \beta_k + \varphi_{ik} \end{gathered} \tag{2-14}$$

where β_{ik} is the parameter of the kth explanatory variable for a spatial unit (curve segment) i, β_k is the mean parameter across all observation, and φ_{ik} is a randomly distributed term with an analyst-specified distribution (like normal distribution with mean 0 and variance σ_k^2) that describes unobserved heterogeneity. If some of the variances of the distribution is tested as not significantly different from zero for a certain explanatory variable, the conventional fixed-parameter across all observations is statistically appropriate. If the constant term is the only random parameter, a random parameter model is equivalent to a random effect model.

In most cases, observations are structured to analyst-specified groups to capture heterogeneity among groups for random parameter models, and φ_{ik} can be rewritten as φ_{gk}, where φ_{gk} is a group-specific random term that generates unobserved heterogeneity across groups in response to the kth explanatory variable (Mannering et al. 2016). Namely, an analyst-specified group shares the same random term for explanatory variables

2.3.2 Geographically Weighted Regression (GWR)

To deal with spatial non-stationarity, a GWR approach was considered in this thesis. The basic model to interpret spatial heterogeneity problems is the GWPR model developed by Nakaya et al. (2005), which allows estimated regression parameters to vary over space. The following framework forms the model:

$$ln(\lambda_i) = \beta_0(u_i) + \sum_{k=1}^{p} \beta_k(u_i) X_{ik} \tag{2-15}$$

where the estimated coefficients β_k are determined by location u_i = (u_{xi}, u_{yi}) denoting curve segment midpoint coordinates, and implies that the parameter β_k varies among the curve segments.

The parameters matrix for each spatial unit are estimated as follows:

$$\hat{\beta}(u_i) = (X^T W(u_i) X)^{-1} X^T W(u_i) Y \tag{2-16}$$

where $\hat{\beta}(u_i)$ is local regression coefficients for the spatial unit i, X is the design matrix of the explanatory variables, X^T is the transposed X, Y is the dependent variables, and $W(u_i)$ denotes an $n \times n$ spatial weighting matrix which is defined as:

$$W(u_i) = diag(w_{i1}, w_{i2}, \cdots, w_{in}) \tag{2-17}$$

where $w_{ij}(j = 1,2, \dots, n)$ is the geographical weight of the j th observation at the i th regression point. In GWR approach theory, estimating the parameters of each regression point is based on the other observations within an appropriate bandwidth. These nearby observations are assigned weight according to the distance from the observations to the regression point in the regression process. For each regression point, the observations located from the edge of the bandwidth to the regression point would yield more weight. The weight w_{ij} is commonly calculated by two types of conventional kernels, i.e., the Gaussian and the bi-square (adaptive) functions, which are defined as follows:

$$\text{Gaussian: } w_{ij} = exp\left(-0.5 \frac{d_{ij}^2}{b^2}\right) \tag{2-138}$$

$$\text{Adaptive bi-square: } w_{ij} = \begin{cases} (1 - (\frac{d_{ij}^2}{b_{i(k)}}))^2 & d_{ij} \le b_{i(k)} \\ 0 & d_{ij} > b_{i(k)} \end{cases} \tag{2-19}$$

where d_{ij} is the distance between neighbor observations i and j, b is the fixed bandwidth, and $b_{i(k)}$ is an adaptive bandwidth size defined by the k-th nearest neighbor distance (Fotheringham et al. 2003). The bandwidth is constant in the Gaussian function (fixed kernel), while the bandwidth of the adaptive bi-square function varies in response to the sample location density.

AICc, which is AIC with a correction for small sample sizes, is applied to select the optimum bandwidth and model comparison illustrated in the next section. The lower AICc a model can generate, the better performance it provides (Fotheringham et al. 2003; Nakaya et al. 2005; Hadayeghi et al. 2010a).

Similar to traditional count models, violation of the Poisson distribution also happens when the variance differs from the mean. The NB form is also applied to the GWR approach to account for the over-dispersion problem. Silva and Rodrigues (2014) developed an algorithm to model over-dispersed data in a non-stationary way by GWNBR. The proposed GWNBR model is defined as:

$$ln(\lambda_i) = \beta_0(u_i) + \sum_{k=1}^{p} \beta_k(u_i) X_{ik} + \theta_i \quad (2\text{-}20)$$

where gamma-distributed error term e^{θ_i} is the same with Equation 2-12, but only $\alpha(u_i)$ varies over the spatial units. The other terms are as defined in Equation 2-15. A modified Iteratively Reweighted Least Squares procedure is used to estimate the parameters β_k and α. Applying the Newton-Raphson algorithm, a subroutine with the maximum likelihood method can be carried out in this procedure. (Silva and Rodrigues 2014).

Set the predicted mean as μ_i, parameterizing this model in terms of μ_i/t_i, t_i gives the offset variables. Thus, this model can be expressed as $\lambda_i \sim NB[t_i\, exp(\sum_k \beta_k(u_i)\, X_{ik})\,, \alpha(u_i)]$ or $\lambda_i \sim \mathrm{NB}[\mu_i, \alpha(u_i)]$. The parameter vector for each spatial unit is determined by:

$$\hat{\beta}(u_i) = (X^T W(u_i) A(u_i)^{(m)} X)^{-1} X^T W(u_i) A(u_i)^{(m)} z(u_i) \quad (2\text{-}21)$$

where $A(u_i)^{(m)}$ is an $n \times n$ GLM diagonal weighting matrix for iteration m, and locations i, $z(u_i)$ are the adjusted dependent variables. The other terms are as defined earlier in the GWPR model. The effective number of parameters of the GWNBR (k) can be calculated by adding the effective numbers of parameters in response to β and α.

To simplify the calculation of GWNBR, GWNBRg introduces a global over-dispersion parameter. It can be noted as $\lambda_i \sim NB[t_i\, exp(\sum_k \beta_k(u_i)\, X_{ik})\,, \alpha]$ or $\lambda_i \sim NB[\mu_i, \alpha]$, where the parameters are the same as in GWNBR. The estimation of the over-dispersion parameter in GWNBRg is the same as that obtained from the non-spatial NB model. Because there is no spatial variation for α, the effective number of parameters contributed from α equals 1.

2.4 Model evaluation methods

2.4.1 Measures of goodness of fit

To provide the average magnitude of the variability of prediction, the median absolute deviation (MAD) is employed:

$$MAD = \frac{1}{n} \sum_{i=1}^{n} |\hat{y}_i - y_i| \quad (2\text{-}22)$$

where n is the number of observations (i.e., the number of curve segments in this research), and $\hat{y}_i$ is the predicted crash frequency and y_i is the observed crash frequency. The smallest value of MAD is the best result in prediction.

Another goodness of fit measure, AIC_c, was also adopted to consider the model complexity as follows:

$$AIC_c = D + 2K + \frac{2K(K+1)}{n-K-1} \tag{2-23}$$

where D represents the deviance, K is the number of parameters estimated in the model, n is the number of observations. The deviance of the Poisson regression model can be expressed as in (Greene 2011):

$$D = 2\sum_{i=1}^{n}\left[y_i ln\left(\frac{y_i}{\hat{\lambda}_i}\right) + (\hat{\lambda}_i - y_i)\right] \tag{2-24}$$

With regard to spatial regression estimation, the number of parameters is replaced to the effective number of parameters, which can be defined as in (Fotheringham et al. 2002):

$$K = trace(S) \tag{2-25}$$

where matrix S is computed by (Nakaya et al. 2005):

$$S = X(X^T W(u_i)A(u_i)X)^{-1}X^T W(u_i)A(u_i) \tag{2-26}$$

The model with the minimum AIC_c value is considered to have the best goodness of fit among the candidate models.

2.4.2 Spatial autocorrelation

Spatial autocorrelation is a basic theory in spatial analysis that can be quantified with indices. From a microscopical perspective, it represents the correlation among adjacent observations on a two-dimensional surface. From a macroscopical perspective, it describes how mapped variables with similar values are clustered, randomly distributed, or dispersed. Features with similar values tend to cluster together, and positive spatial autocorrelation occurs; when they distribute dispersedly, negative spatial autocorrelation occurs.

One of the most widely applied indexes is the Moran Global Index (Moran's I) (Moran 1950), which can be expressed as follows:

$$I = \frac{n\sum_{i=1}^{n}\sum_{j=1}^{n} w_{i,j}(r_i - \bar{r})(r_j - \bar{r})}{S_0 \sum_{i=1}^{n}(r_i - \bar{r})_i^2} \tag{2-27}$$

$$S_0 = \sum_{i=1}^{n}\sum_{j=1}^{n} w_{ij} \tag{2-28}$$

where n is the number of spatial units indexed by i and j, $w_{i,j}$ is the spatial weight between unit i and unit j, r is the residual of model for each unit, and $\bar{r}$ is the mean of r. Moran's I value varies

between -1 to 1, where 0 indicates perfect random spatial distribution. However, only when the p-value is statistically significant (p-value$\leq$ 0.05) can the null hypothesis be rejected. A positive value implies similarity among the neighbors and the residuals are concentrated, while a negative value means discrepancy among the neighbors and the residuals are dispersed. In summary, the higher the absolute value Moran's I is, the stronger the spatial autocorrelation data.

3. DATA COLLECTION

3.1 Crash data

Crash data for the state of Indiana was utilized in this thesis to evaluate the proposed HFST safety performance and different models. The data, which was collected during 2016 through 2018 and includes all U.S. and state highways in Indiana, was retrieved from the Automated Reporting Information Exchange System (ARIES) portal. As there are commonly errors in GPS coordinates recorded by police officers (Imprialou et al. 2019), this thesis applied the CLIP software developed by the Purdue University Center for Road Safety (Romero et al. 2017) to correct crash occurrence locations by geocoding the position description for each crash record.

The horizontal curve segments were generated as the primary data. To do so, the road network database provided by the FHWA Highway Performance Monitoring System (HPMS) was used to detect and extract horizontal curve segments using the ROCA (ROad Curvature Analyst) tool in ESRI ArcGIS (Bíl et al. 2018). Figure 3.1 shows the statewide curve segment distribution and two typical road curve identification examples at the plain areas and the hilly areas. Out of the entire 17,381 km Indiana road network for Indiana state routes and U.S. highways, 1,545 km curve segments were identified and adopted as the base units. Four independent variables were selected for crash count modeling; and among them, the radius and length of each curve were calculated using the ROCA software as the geometric variables. Although the curve radius and length were designed according to a certain correlation in the planning process, in this thesis, the curve segments were identified from the road network shapefile, meaning that the length of a curve segment was not correlated with its radius, i.e., the correlation coefficient between them was 0.337.

The third independent variable considered was pavement friction. The pavement friction data, which was measured at 40 mph with standard smooth tires, was retrieved from INDOT's network pavement friction database.

The fourth independent variable was AADT. The AADT shapefiles between 2016 and 2018 were downloaded from the INDOT traffic flow website, where the road sections having relatively uniform travel characteristics are assigned the same value.

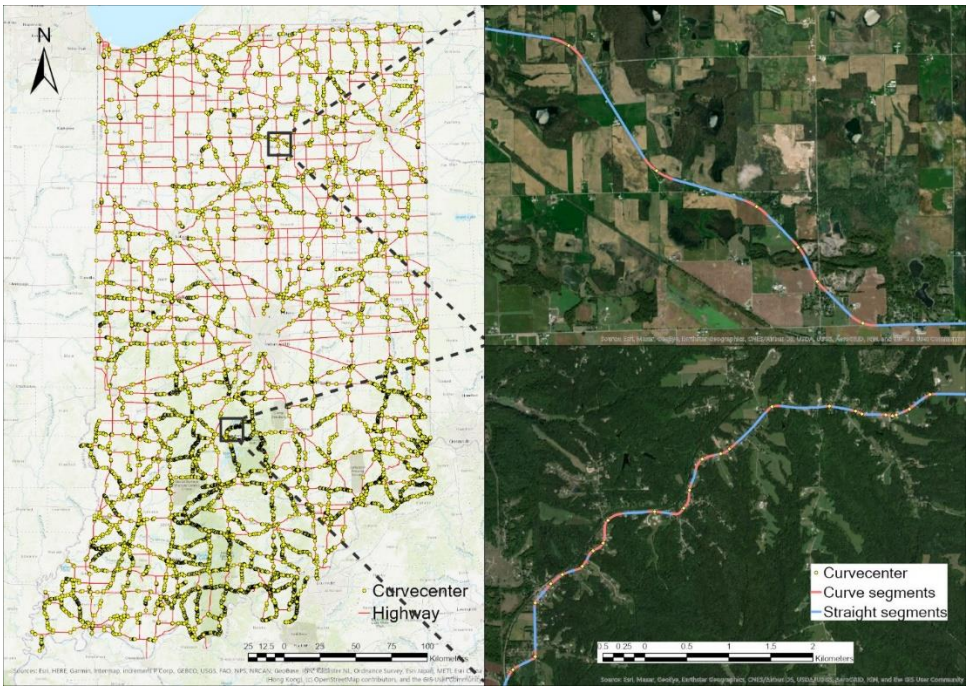

Figure 3.1. Curve segments distribution in Indiana (left) and typical examples on SR-114 (upper right) and SR-450 (lower right).

Crashes were filtered with a horizontal curve segment 50 m buffer. The crash counts were totaled for three years of crash frequency for each curve segment. The curve segments were aggregated with the nearest pavement friction shapefile and the AADT shapefile using ArcGIS.

Table 3.1. Variable description and summary statistics of micro-level dataset.

Variables	Description	Mean	Std. dev	Min	Max
N	Number of crashes occurred during 2016-2018 per curve segment	0.740	1.755	0	34
$R\ (m)$	Radii of curve segments in meter	354.10	199.61	25.21	999.64
F	Friction of pavement on curve segments at 40 mph	43.80	15.12	8.2	104.2
$L\ (m)$	Length of curve segments in meter	104.05	109.92	30.49	1249.77
A	Mean of AADT in 2016-2018	4214.16	5393.82	32.21	82,244.85

The variables used for micro-level model specification and their descriptive statistics are summarized in Table 3.1. Because a closer linear relationship with the dependent variable was observed on the logarithmic scale, logarithmic transformation was applied to the independent variable. The VIF was employed to assess the multicollinearity among the variables in the data;

and the VIFs of all the variables had values lower than two, indicating that there was no significant multi-collinearity (Heiberger and Holland 2015).

To model crash frequency at the macro level, the crashes were counted for all 92 counties in Indiana because the county level is the lowest zonal level at which each county has highway road segments located; and the spatial model weight matrix calculations were based on their centroid coordinates. Because the INDOT highway network used in this thesis does not include all the state's highways, the highway curve segment crash frequency was intuitively irrelevant to the demographic and climatic variables. Therefore, the exposure parameter of yearly VMT per county was considered a major influential variable. Given that the average curve radius and pavement friction of each county would not show any significance in this model, it was reasonable to split the total VMT into VMTs for different type of curve segments by their radius and friction to analyze their influence. The variables used for micro-level model specification and their descriptive statistics are summarized in Table 3.2. Referring to Musey (2017), the horizontal curves were classified as follows:

gentle curve: radius > 350 m; sharp curve: radius < 350 m

low friction curve: friction < 40; high friction curve: friction > 40

Table 3.2. Variable description and summary statistics of micro-level dataset.

Variables	Description	Mean	Std. dev	Min	Max
N	Number of crashes occurred during 2016-2018 per county	75.71	54.73	2	256
VMT_gh	Total yearly VMT of high friction gentle curve segments	5.59	4.34	0.33	21.08
VMT_gl	Total yearly VMT of low friction gentle curve segments	5.48	5.01	0	24.11
VMT_sh	Total yearly VMT of high friction sharp curve segments	2.19	1.95	0.06	9.78
VMT_sl	Total yearly VMT of low friction sharp curve segments	2.93	2.62	0.06	11.04

Note: VMT value is in million miles

3.2 HFST information

To obtain the most precise HFST pavement segment shapefiles, digitization was conducted to record their satellite images and construction information. These images, which were published in 2014 with a pixel size of 3 m, was obtained from the National Agriculture Imagery Program (NAIP). Overall, 3.696 miles of 25 HFST pavement segments were digitized for crash counting. Crash data was collected during 2016 through 2019 occurred within 25 meters of the centerline of

an HFST curve segment. The crash data before HFST installation is for year 2016 to 2018, while the post HFST crash data covers year 2019. Not including the crash data for year 2020 is a result of unusual traffic volume during COVID-19 pandemic. The decreasing number of crashes in 2020 would likely be not due to HFST. Table 3.3 shows the detailed crash counts and other information about each HFST site. Figure 3.2 shows the geographical locations and digitization of the HFST sites.

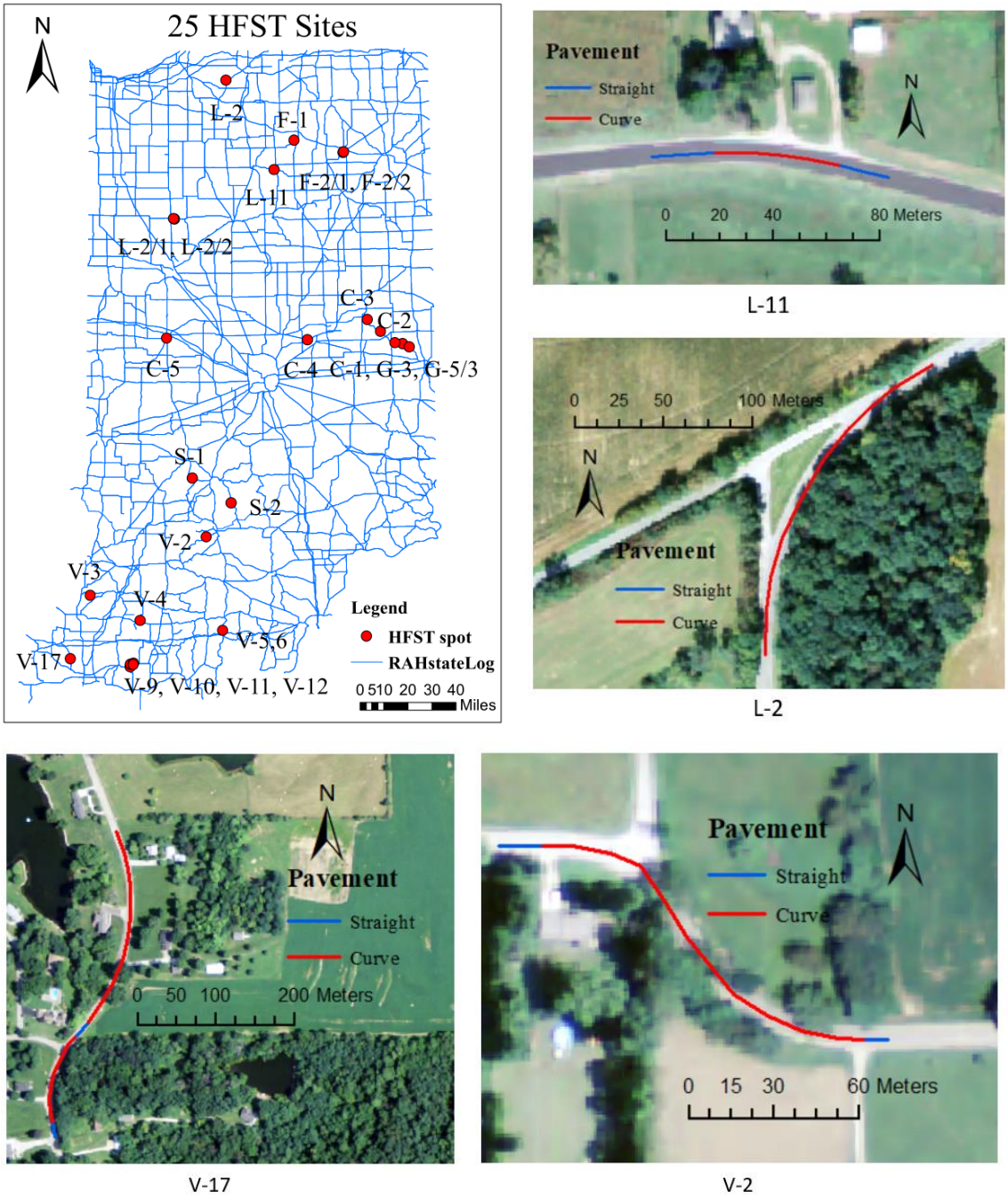

Figure 3.2. HFST installations in Indiana.

Figure 3.2. Continued

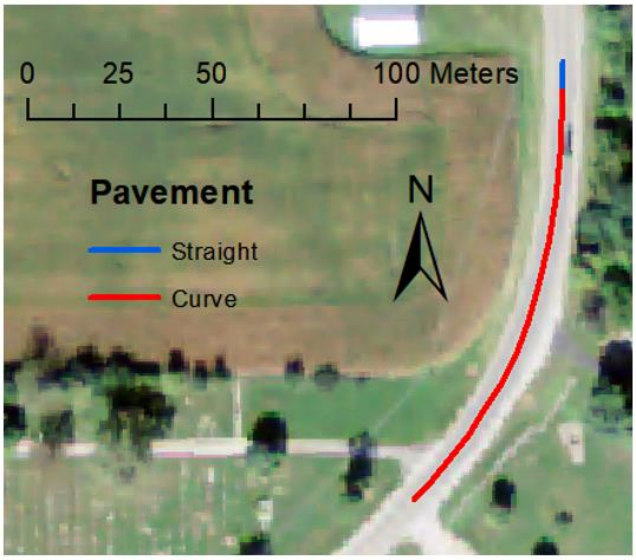

F-2/1

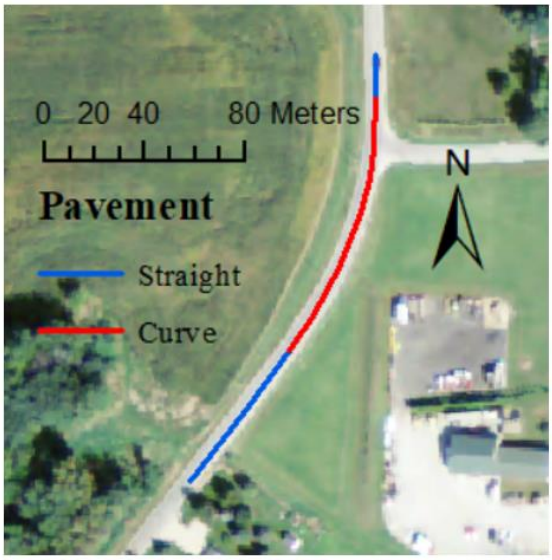

F-1

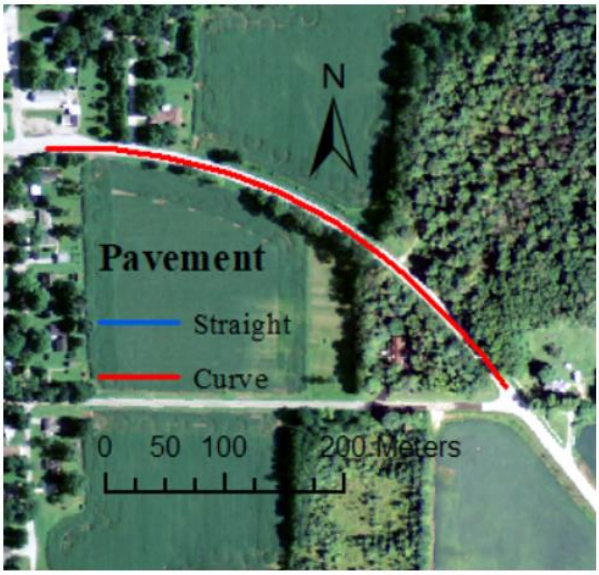

G-5/1

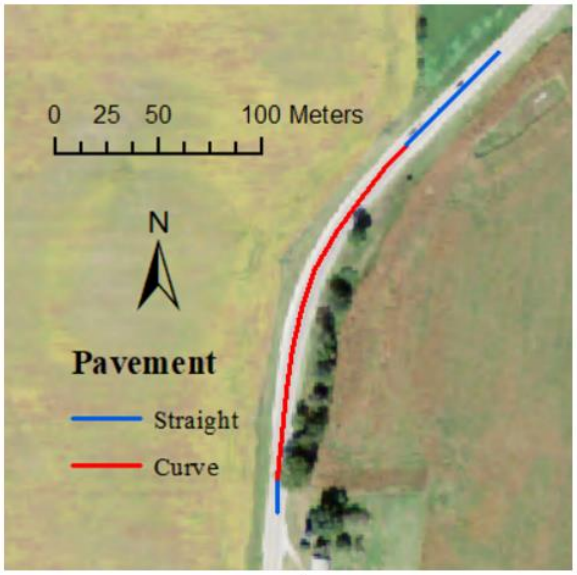

F-2/2

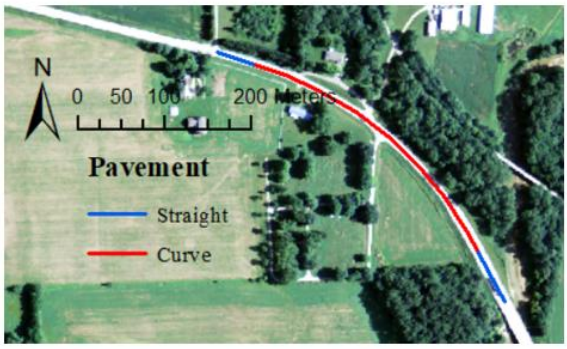

G-5/3

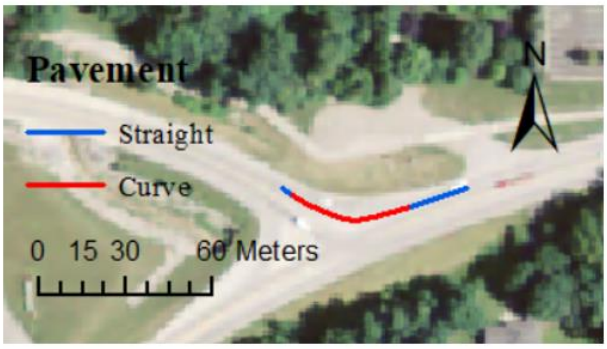

C-5

Figure 3.2. Continued

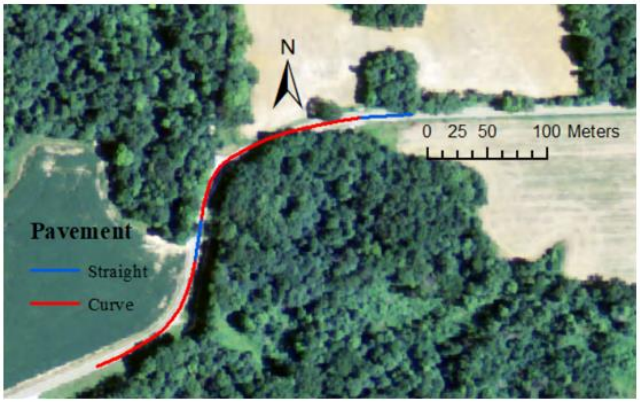

V-3

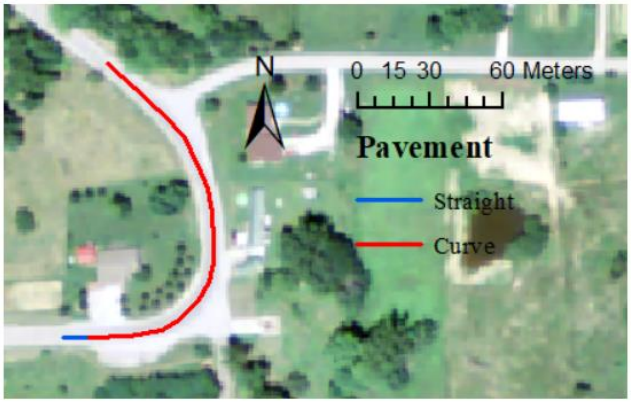

V-4

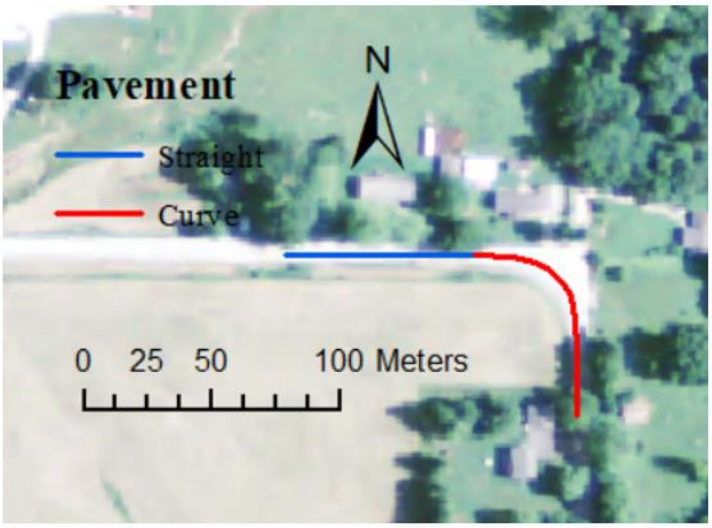

S-1

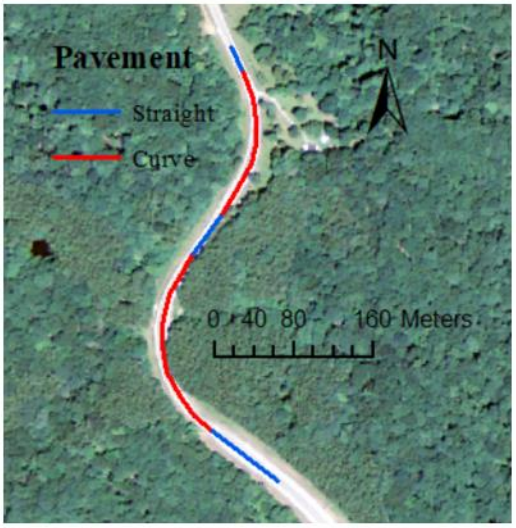

S-2

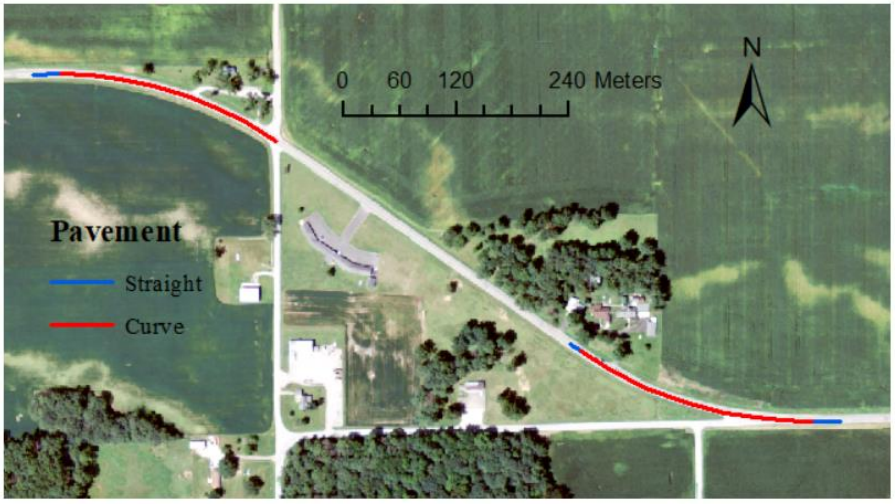

L-1/2 L-1/1

Figure 3.2. Continued

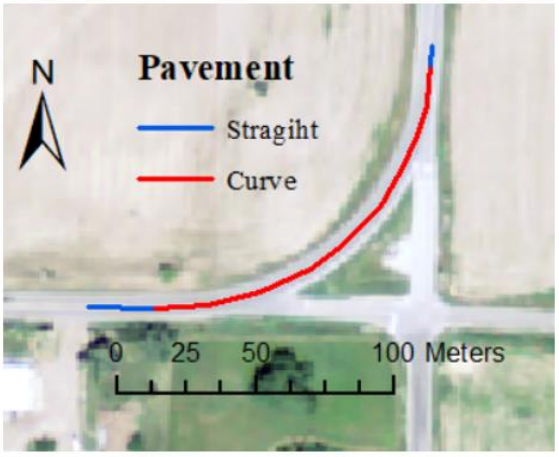

V-9

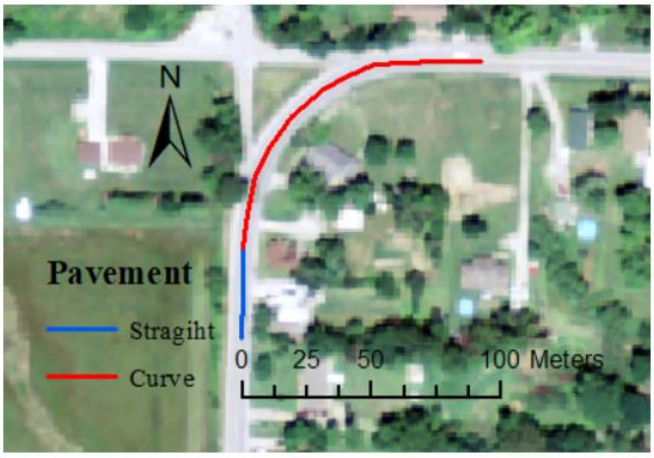

V-10

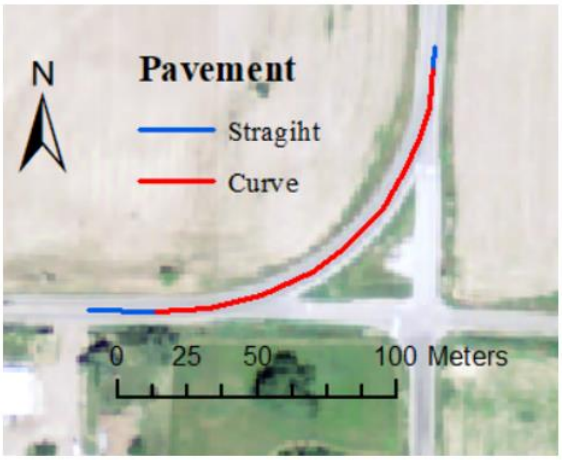

V-11

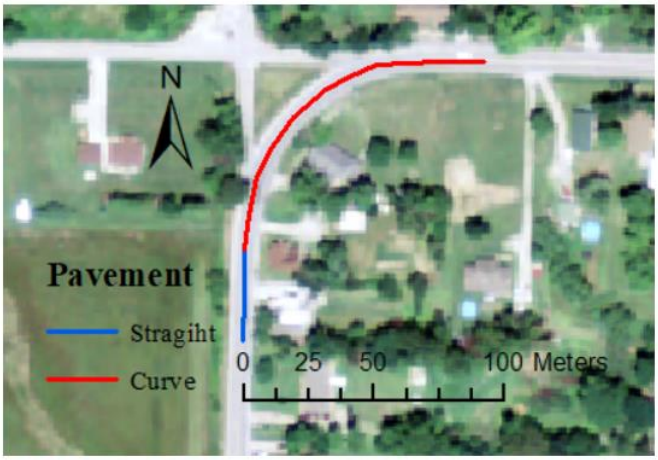

V-12

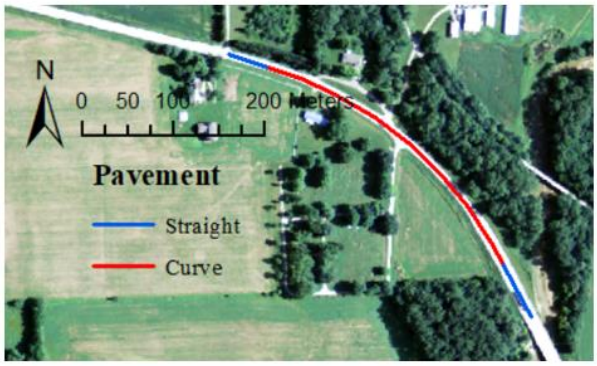

G-5/3

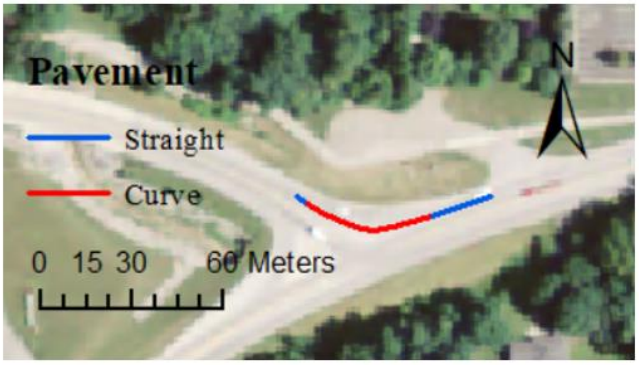

C-5

Figure 3.2. Continued

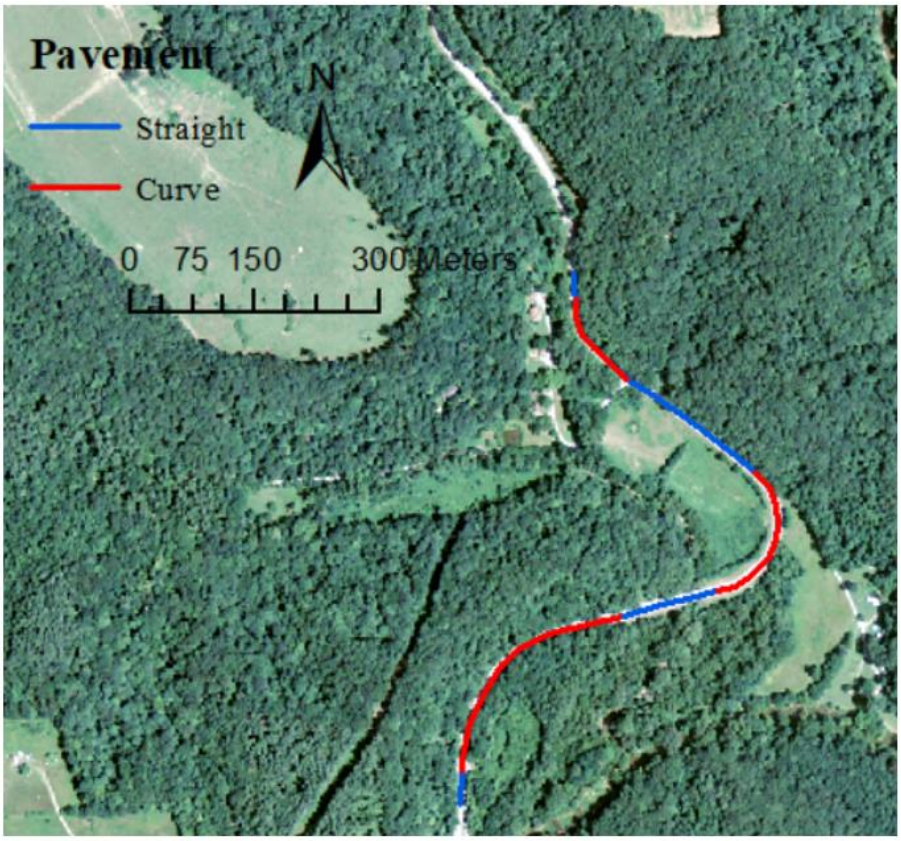

V-5,6

Table 3.3. Indiana HFST site before (2016-2018) and after (2019) crash counts.

HFST Site	Length (mile)	FN@40 mph		Wet Weather Crashes		Injury Crashes		All Crashes	
		Before	After	Before	After	Before	After	Before	After
F-1	0.25	34.9	81.5	9	0	6	0	16	3
F-2/2	0.157	31.7	79.8	1	0	0	0	2	0
G-5/3	0.28	35.2	93.1	0	0	0	0	0	0
L-1/2	0.18	25.1	81.2	2	1	1	0	6	2
L-1/1	0.16	26.0	84.9	4	1	2	0	10	1
L-2	0.11	47.5	82.7	0	1	0	0	1	1
V-17	0.21	52.4	84.4	1	0	0	0	2	0
V-2	0.14	23.1	75.3	1	0	1	0	2	1
V-4	0.15	23.4	72.3	0	0	0	0	0	0
V-5,6	0.61	38.1	87.6	2	0	1	0	3	0
V-9	0.1	44.5	82.4	0	0	1	0	2	1
V-10	0.11	46.7	81.9	0	0	3	1	7	3
V-11	0.13	51.5	84.0	0	0	0	0	0	0
V-12	0.11	52.4	88.2	0	0	0	0	3	0
V-3	0.14	53.5	86.0	0	0	0	0	1	0
L-11	0.05	24.3	87.1	2	0	0	0	2	0
S-1	0.09	28.6	67.9	1	1	1	0	3	1
S-2	0.33	19.9	83.1	2	0	1	1	3	2
F-2/1	0.08	29.1	81.2	4	0	0	0	4	0
C-1	0.17	42.2	87.2	0	0	0	1	0	1
C-2	0.06	52.3	87.2	1	0	1	0	3	0
C-4	0.06	52.3	85.9	3	3	3	1	17	5
G-3	0.2	41.1	88.9	2	0	1	0	4	0
C-5	0.049	44.5	71.2	1	0	1	0	1	1
C-3	0.17	43.8	87.7	1	0	1	0	6	1
Sum	4.096	-	-	37	7	24	4	98	23

4. RESULTS AND EVALUATION

This chapter presents the evaluation of 25 HFST sites in Indiana as well as a comparison conducted with other state results. The local analysis and findings for the specific micro-level GWNBR model then are presented to conclude the chapter.

4.1 Analysis of before-after HFST

Since estimating CMFs is not a trivial task, the estimate in this evaluation is an approximation that applies to an ideal comparison group with yearly trends identical to the treatment group, which is a highly unlikely situation. Therefore, this thesis recognizes that this estimate could be a conservatively low approximation. The results of the EB analysis of the CMFs for all 25 HFST sites are shown in Table 4.1.

Table 4.1. Aggregated CMF results for Indiana HFST sites.

Crash Type	Observed Crash After	EB Expected After	CMF (std. dev)
Total	23	31.93	0.701 (0.184)
Injury	4	7.87	0.496 (0.195)
Wet weather	7	11.61	0.563 (0.172)

As shown in Table 4.1, the estimate of the HFST CMFs using the EB method was 0.701 with a standard deviation of 0.184. A key feature of the EB method is that it reduces uncertainty in CMF estimates because it uses more information and a more rigorous methodology. There have been HFST CMF research studies in other states (see Table 4.2). A comparison of the results of this thesis with those studies revealed that the HFSTs installed in Indiana demonstrated a safety impact well within the proven range found by other states.

Table 4.2. Estimated HFST CMF value comparison with other states.

Crash Type	Indiana	CMF by Merritt et al. (2015) (CO, KS, KY, MI, MT, SC, TN)	CMF by Lyon et al. (2020) (PA, WV, KY, AR)
Total	0.701	0.759	0.428
Wet weather	0.563	0.481	0.167

4.2 Macro-level crash frequency modeling

Macro-level modeling was estimated by Poisson and GWPR, as the over-dispersion showed no significance. A GWPR model was implemented using GWR4 software (Nakaya et al. 2009).

4.2.1 Model estimation

The optimum AICc of the global Poisson model was 829.67 while the optimum AICc of the GWPR model was 627.53, indicating that the GWPR model presented better goodness of fit over the Poisson model. The lowest AICc was searched through a bandwidth of a fixed Gaussian and adaptive bi-square kernel function, and the fixed Gaussian bandwidth of best performance was 61807 m. The effective number of parameters of the GWPR model was 25.0, which indicated an extension of the parameters from the Poisson model. When the RPNB model was applied for potential heterogeneity, none of these parameters were shown to be significant on the variance of the random parameter.

The results of the local parameters are described by the 5-number summaries, which represent the minimum, lower quartile, median, upper quartile, and maximum values in Table 4.3. From Table 4.3, it can be seen that the mean coefficients of the GWPR model were close to the Poisson coefficients. All four variables showed positive signs in the Poisson model, indicating that increasing the VMT always resulted in more crash occurrence. The coefficients of the sharp curve VMT were higher than the gentle curve VMT, which matched the assumption of this thesis. However, friction did not show a similar pattern on the gentle and sharp curves, reflecting that friction may not play an important role on the safety performance of gentle curves. Note that there was a counterintuitive sign on the minimum value of $log\ (VMT_{gh})$, as its overall coefficients were close to zero. However, the t-values of observations with a negative sign all were lower than 1.984, meaning that their confidence level of significance was lower than 97.5%.

To quantify the change in the model residual spatial autocorrelation, Moran's I statistics were calculated for both models. The Moran's I of the Poisson model was 0.1857 with a p-value of 0.00, indicating that the counties with similar residuals were clustered. The Moran's I of the GWPR model was -0.0319 with a p-value of 0.708, which was a large improvement from the non-spatial model. However, the p-value of the Moran's I significance did not reach the 90%

confidence level so it could not be concluded yet that the GWPR model's residuals were randomly distributed over all 92 counties.

Table 4.3. Estimated parameters of Poisson and GWPR models.

Model	Poisson	GWPR					
		Mean	Min	Lwr	Med	Upr	Max
Intercept	3.376	3.312	2.428	3.266	3.359	3.436	3.547
$log\ (VMT_{gh})$	0.219	0.254	0.090	0.168	0.240	0.323	0.587
$log\ (VMT_{gl})$	0.122	0.121	-0.045	0.060	0.135	0.177	0.320
$log\ (VMT_{sh})$	0.229	0.247	0.065	0.167	0.231	0.330	0.399
$log\ (VMT_{sl})$	0.300	0.278	0.059	0.231	0.288	0.333	0.408

4.2.2 Model interpretation

The distributions of the 92 Indiana counties' coefficient estimates and their t-values are shown in Figure 4.1 and Figure 4.2, respectively. An obvious nonstationary spatial pattern of parameters can be seen in these figures. The observations with significant coefficients were VMT_{gh}, VMT_{gl} , VMT_{sh}, and VMT_{sl}, which accounted for 95.7%, 77.2%, 94.6%, and 96.74%, respectively. The GWPR model was able to capture the spatial heterogeneity between the frequency of the curve crashes and the explanatory variables, which was hidden in the Poisson model.

Figure 4.1 and Figure 4.2 also show a clear established pattern. For the gentle high friction curve VMT, the parameters gradually decreased from the eastern counties to the other counties, except for the southwest corner counties. As the safest type of road, the high coefficients of VMT_{gh} may reflect that factors other than friction and radius were influencing highway curve safety in those counties. Only four counties in the lakeshore area did not show significance at 99% confidence level for this variable. With respect to the gentle low friction curve VMT, the mean coefficient was similar with its small value in the global Poisson model. A total of 21 eastern counties showed low significance, and the other counties' values decreased to the east. This result indicates that to improve curve safety, the counties with high coefficients may require new installations of HFST. The sharp high friction curve VMT coefficient distribution shows a trend of decreasing from the center belt to the north and the south. Only three counties in the northeast and Posey County in the southwest showed low significance. Flattening curves could be a helpful implementation to improve traffic safety for the counties in the "high coefficient belt." The most

high-risk type of curve, i.e., sharp low friction, showed the highest value for the central northern to eastern counties. Two counties on the west edge and one county on the northeast corner had a significance confidence level lower than 99%, which indicated that those counties with a high coefficient need to pay more attention to their low friction sharp curves from a safety perspective. In summary, this model's results provide suggestions as to which counties INDOT should focus on when trying to improve the safety on certain types of highway curves.

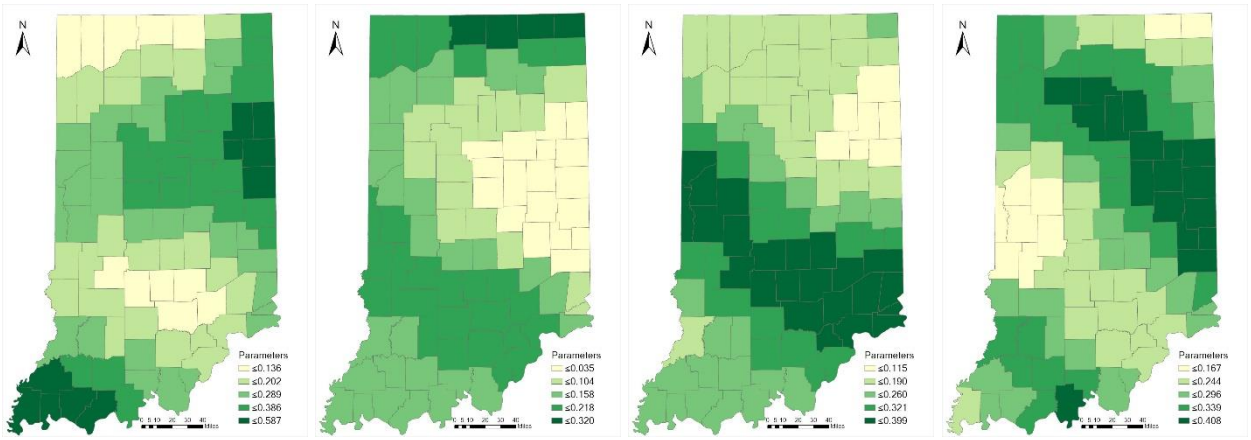

(a) (b) (c) (d)

Figure 4.1. Coefficient distribution of (a) gentle high friction curve VMT, (b) gentle low friction curve VMT, (c) sharp high friction curve VMT, and (d) sharp low friction curve VMT.

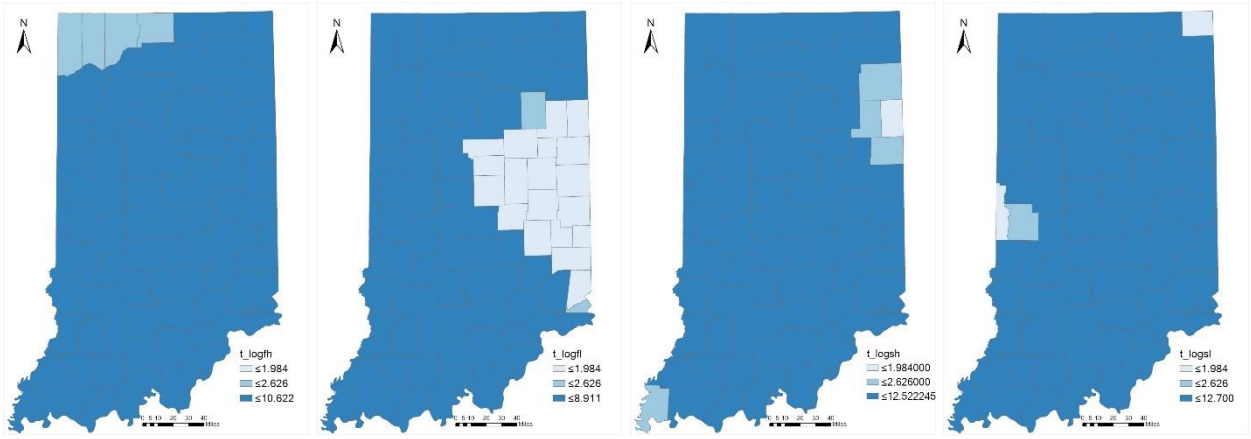

(a) (b) (c) (d)

Figure 4.2. The *t* value of (a) gentle high friction curve VMT, (b) gentle low friction curve VMT, (c) sharp high friction curve VMT, and (d) sharp low friction curve VMT.

4.3 Micro-level crash frequency modeling

The micro-level modeling of this thesis was estimated using both spatial (GWPR, GWNBR, and GWNBRg) and non-spatial (NB, ZINB, and RPNB) models in conjunction with the dataset described in Chapter 3. The estimation of the RPNB model and the GWR approach were performed by NLOGIT6 and Golden macro in SAS®9.4 (Silva et al. 2016), respectively.

4.3.1 Model comparison

As the crash frequency studied in this thesis occurred between 2016 and 2018 showed a significant over-dispersion parameter (1.88), an NB model was proposed as the basic conventional nonstationary model with which to begin the process. Other than the over-dispersion that was exhibited by the micro-level dataset, another characteristic was its "inflated" zero count observations. A total of 6,329 curve segments out of 9,415 did not experience any crashes in those three years. A ZINB model was then specified, which resulted in a Vuong statistic of 3.313; and this value was greater than 1.96, meaning that the ZINB model outperformed the traditional NB model. All the parameters were significant in the zero state except friction, which indicated that friction was not a dominant factor in determining the likelihood of these curve segments to ever suffer any events.

We estimated the RPNB model by using the normal distribution as a parameter density function, which was accomplished using 100 Halton plots of simulation-based maximum likelihood. This model was applied to account for the heterogeneity among the individual curve segments in order to compare its results with the GWR approach that assumes the parameters vary among the curve segments. Although specifying groups in random parameter models is popular, as mentioned earlier, there was no need to divide the data into groups in this thesis.

For the GWR approach, a fixed Gaussian function was applied as the kernel function curve segments were identified from the road network. Assuming that the unobserved heterogeneity of curve crashes resulted from climate, terrain, and driver behavior, their spatial correlation matrix was assumed to be independent of the number of neighbors. Thus, the bandwidth was set to be Gaussian fixed kernel functions as defined in Equation 2-18, and the distance between a pair of curve segments' midpoints was set as the Euclidean distance in the kernel function. Moreover, the

optimum bandwidths with the lowest AICc for the GWR approach were selected using the SAS Golden macro.

The results of the model estimations are presented in Table 4.4. Several general observations are worth noting. The GWNBR model produced the lowest AICc value and the highest log likelihood value, which indicated that by accounting for the spatial heterogeneity of all the variables and dispersion parameters, the curve crash frequency was depicted best by the GWNBR model. The RPNB model had a larger AICc value than the ZINB model, implying that even a non-stationary model without addressing the spatial factors could outperform an advanced stationary model. Concerning the MAD metric, the GWPR model surprisingly observed a smaller MAD value than the GWNBR model. One explanation for this result is that the GWPR model with the smallest MAD tended to have a bandwidth much smaller than that of the GWNBR model. A smaller bandwidth size allowed the GWPR model to depict local varying parameters while making it less vulnerable to extreme values. Furthermore, the RPNB and GWNBRg models had similar performances for log likelihood and AICc, wherein both assumed that the dispersion parameter did not vary over space. Finally, the traditional NB model, as expected, performed worst for every goodness of fit measure.

Table 4.4. Goodness of fit and residual spatial dependency for different models.

Model	Bandwidth (km)	# of parameter	MAD	Log likelihood	AICc	Dispersion Parameter	Moran's I	p-value
NB	-	5	0.881	-9,978.4	19,968.0	1.88	0.1542	10^{-43}
ZINB	-	9	0.878	-9,950.0	19,918.2	1.39	0.1553	10^{-44}
RPNB	-	11	0.847	-9,917.1	19,856.2	1.31	0.0753	10^{-41}
GWPR	15.45	295.1	0.845	-10,805.9	22,219.9	-	0.0297	10^{-7}
GWNBR	34.65	76.5	0.859	-9,780.7	19,715.6	-	0.0569	10^{-24}
GWNBRg	76.01	22.7	0.869	-9,900.9	19,847.4	1.88	0.0634	10^{-30}

Note: p-value is the possibility of model residual random distribution over space

To quantify the spatial autocorrelation of the predicted residuals for these models over curve segments, Moran's I was employed. The results are presented in Table 4.4.

The Moran's I results show that the non-spatial models (NB, ZINB, and RPNB) always had a higher value than the GWR model, which reflected a relatively high spatial autocorrelation without considering spatial variation. The GWPR, GWNBR, and GWNBRg models showed

decreasing Moran's I values, which may be related to their different optimum bandwidth (GWPR<GWNBR<GWBNRg), i.e., the local patterns depicted from the model strongly reduced residual prediction autocorrelation. However, none of these models showed significance for the non-autocorrelation of the prediction residuals. Table 4.4 shows that the reduction of the residual autocorrelation from the NB to GWNBR models had 99% significance, indicating that the GWNBR model was capable of producing a relatively non-biased estimation compared to the global model.

4.3.2 Statistics of estimated parameters

The estimated parameters are summarized in Table 4.5. The parameters are denoted as LOGR, LOGL, LOGF, and LOGA, representing the logarithms of radius, length, friction, and AADT, respectively. The local parameters in the RPNB and GWR models were described by the minimum, lower quartile, median, upper quartile, and maximum of values, while only the point estimation of the coefficients in the NB model was provided. The parameters of the global NB model showed positive signs for curve length and traffic volume (LOGL and LOGA), which indicated that crash frequency rose with an increase in the curve segment length and the traffic count. The estimations of the curve radius and pavement friction (LOGR and LOGF) showed negative global parameters, which made sense and agreed well with recent research findings (Geedipally et al. 2019, Himes et al. 2019). All the parameters in the normal state of the ZINB model showed identical signs with the NB model but had a smaller absolute value than the NB model as its zero state explained part of the crash occurrence. The signs of the parameters of the ZINB model's zero state showed a different sign from the normal state because it represents the possibility of being qualitatively set as zero state. As shown in Table 4.5, the parameter statistics revealed the following: (1) the mean and median values of the estimated parameters generated from all these non-stationary models were close to that obtained with the global NB model, indicating that the global model generally reflected the average impact of these factors in the non-stationary models; and (2) the range of varying parameters could be ranked as GWPR> GWNBR> GWNBRg> RPNB, which is in agreement with the discussion in the next section.

Table 4.5. Estimated parameters of NB, ZINB, RPNB, GWPR, GWNBR, and GWNBRg models.

Model	NB	RPNB						GWPR					
		Mean	Min	Lwr	Med	Upr	Max	Mean	Min	Lwr	Med	Upr	Max
Intercept	-5.96	-6.25	-6.33	-6.26	-6.25	-6.23	-5.82	-6.14	-22.17	-8.21	-6.00	-4.32	3.56
LOGR	-0.24	-0.30	-0.33	-0.31	-0.30	-0.29	-0.14	-0.23	-1.04	-0.36	-0.24	-0.10	0.61
LOGL	0.87	0.96	0.94	0.95	0.96	0.96	1.07	0.87	0.137	0.68	0.85	1.05	1.98
LOGF	-0.36	-0.40	-0.46	-0.42	-0.41	-0.39	0.08	-0.29	-2.24	-0.44	-0.25	-0.04	0.94
LOGA	0.49	0.48	0.46	0.48	0.48	0.49	0.61	0.47	-0.34	0.35	0.51	0.61	1.24

Model	ZINB		GWNBR						GWNBRg					
	Count	Zero	Mean	Min	Lwr	Med	Upr	Max	Mean	Min	Lwr	Med	Upr	Max
Intercept	-4.31	6.36	-5.80	-9.19	-6.82	-5.64	-5.16	-1.79	-5.82	-7.07	-6.42	-6.01	-5.66	-3.45
LOGR	-0.14	0.52	-0.24	-0.55	-0.30	-0.25	-0.18	0.04	-0.24	-0.33	-0.27	-0.24	-0.23	-0.15
LOGL	0.59	-1.57	0.85	0.46	0.76	0.85	0.93	1.18	0.84	0.73	0.80	0.83	0.87	0.94
LOGF	-0.36	-	-0.31	-0.97	-0.33	-0.28	-0.24	-0.03	-0.33	-0.68	-0.34	-0.30	-0.27	-0.26
LOGA	0.42	-0.38	0.46	0.07	0.36	0.47	0.57	0.73	0.48	0.24	0.40	0.51	0.55	0.60

Note: all parameters in this table are over 99% significance level

It is also worth noting that there were counterintuitive signs in the GWPR and GWNBR models. The GWPR model had counterintuitive signs of coefficients for some observations for the regression intercept and the LOGR, LOGF, and LOGA. The GWNBR model also had a few counterintuitive signs of coefficients for the LOGR. Since the spatial coefficient multicollinearity has been proven not to be responsible for counterintuitive signs (Fotheringham and Oshan 2016), this result can be explained by the hypothesis that some variables may not be significant in certain areas. These local areas may have insignificant counterintuitive signs for some variables (Gomes and Cunto et al. 2017). This can be seen by observing the coefficient spatial distribution of the GWPR and GWNBR models in Figure 4.3. Unexpected significant counterintuitive signs among the variables in the GWPR model could be caused by failing to consider data over-dispersion (Xu and Huang 2015).

4.3.3 Spatial heterogeneity of estimated parameters

The distributions of the local coefficient estimates and their significance interpolated by inverse distance weighted (IDW) for GWPR, GWNBR, and GWNBRg are plotted in Figure 4.3. Using the known parameter values for the 9,415 curve segments, the IDW algorithm predicted the values for the unmeasured locations using the values of the surrounding measured locations. The

areas with a significance level of less than 90% were not considered in the parameter analysis and are shown in gray on the maps. Generally, the coefficient distributions of the GWPR, GWNBR, and GWNBRg models were more homogeneous as a result of their different optimum bandwidths; and the larger their optimum bandwidth was, the more homogeneous their coefficient distributions.

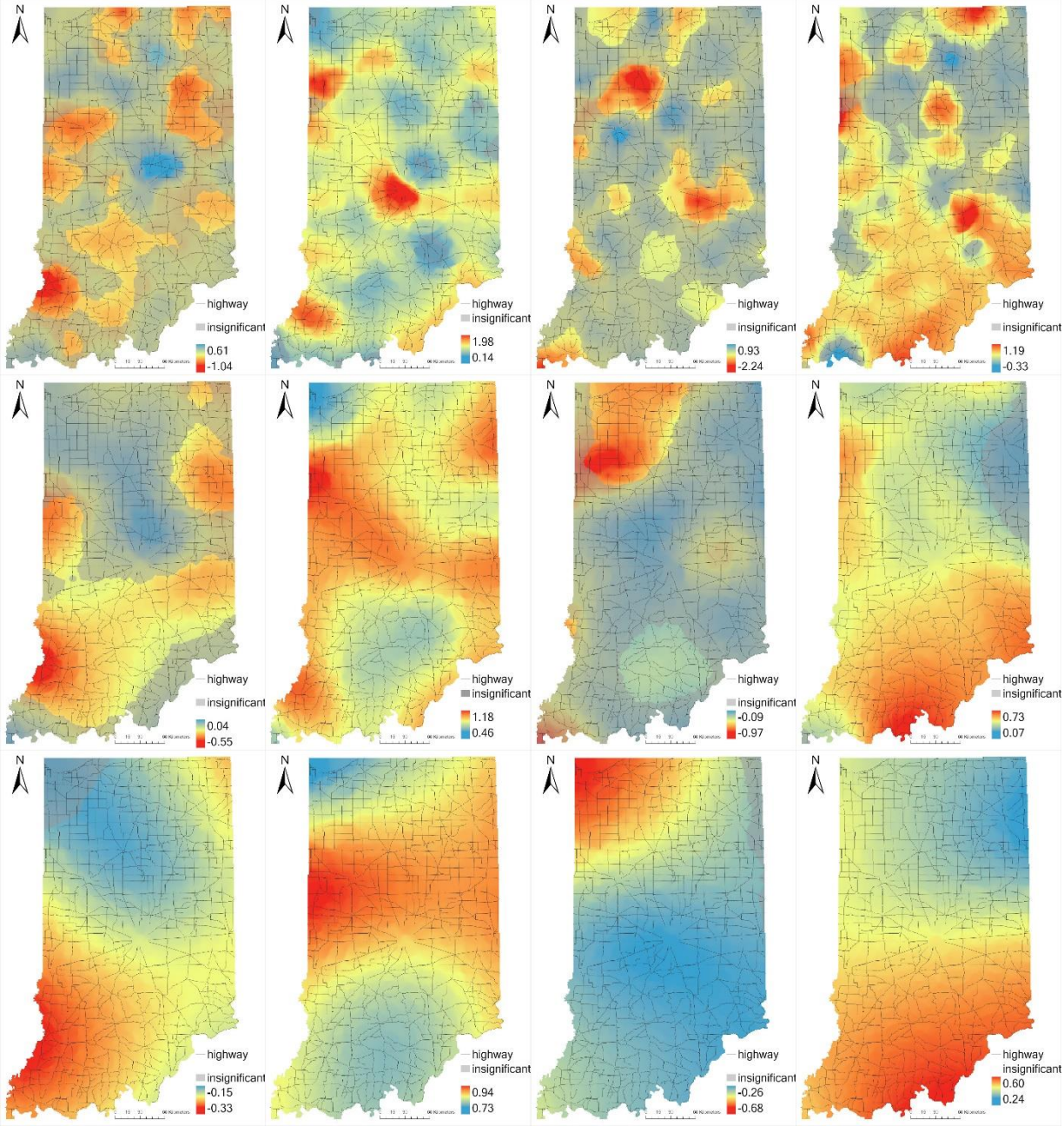

(a)LOGR (b)LOGL (c)LOGF (d)LOGA

Figure 4.3. Distribution of (a) LOGR, (b) LOGL, (c) LOGF, and (d) LOGA in different GWPR (top), GWNBR (middle), and GWNBRg (bottom).

Since the GWNBR model performed best with regard to the goodness of fit in terms of AICc, the parameter estimations are mainly illustrated according to the GWNBR model. Observations with significant coefficients accounted for 54.9%, 100%, 22.0%, and 96.2% for LOGR, LOGL, LOGF, and LOGA, respectively. A high percentage of parameter significance of LOGL and LOGA appeared as expected due to the predominant influence of the exposure factors in crash frequency prediction.

Observing from the curve radius (LOGR) coefficient distribution from the GWPR model in Figure 4.3(a), the central area presented the highest coefficients with only a small area showing positive signs. However, the central and northwestern regions with high coefficients did not present enough significance to be considered in the GWNBR model. The lower values mainly were distributed in the southern part of the state, indicating a significant influence of the curve radius in that region. Figure 4.3(a) also shows several significant regions where it was difficult to summarize the spatial patterns of the radius coefficient for the GWNBR model. The GWNBRg model in Figure 4.3(a) shows a smooth decrease from the northwest to the southwest, which may have been caused by some extreme values. Hence, although 93% of the observations show significant coefficients for the GWNBRg model of LOGR, the coefficient varying trend may not be reliable.

For the curve segment length (LOGL) in Figure 4.3(b), the GWNBR model's coefficient distribution presents two relatively lower coefficient regions in southern Indiana and an area close to Chicago in northwestern Indiana. Similar to the LOGR coefficient distribution, Figure 4.3(b) shows that the GWPR model demonstrated a broken distribution of the LOGL coefficient with no apparent pattern and the GWNBRg model showed a decrease in the coefficient from the central counties to the north and the south.

When analyzing the spatial distribution of the GWNBR model's coefficients for curve friction (LOGF) in Figure 4.3(c), it was observed that there were only two separate regions that showed significant coefficients. For the region located in the southern area that almost coincides with the LOGL southern low coefficient area in Figure 4.3(b), the GWNBR model showed coefficient values of about -0.25, while the other region located in the northern area had significantly lower friction coefficients. Figure 4.3(c) shows that the significant areas were dispersed and further that there was a homogeneous coefficient variation while only northwestern Indiana had low values.

In Figure 4.3(d), the AADT (LOGA) coefficient distribution of the GWNBR model indicated high values in southern and southeastern Indiana as well as a small non-significant coefficient area in northeastern Indiana. Figure 4.3(d) shows that the GWPR model indicated an insignificant coefficient area mainly located in northwestern Indiana. The GWNBRg model (bottom row) indicated a more general coefficient decreasing trend from south to north.

In summary, the coefficient distributions in the GWPR and GWNBRg models identified the disadvantages associated with parameter explanation. All the coefficients displayed a very heterogeneous pattern in the GWPR model while the distribution of the coefficient of the GWNBRg model was very homogeneous. Even without considering the GWPR model having the worst goodness of fit, its coefficient distributions were very detailed for analysis. On the other hand, the GWNBRg model's coefficient distributions showed a statewide smooth surface with small variations, and almost all the observations had significant coefficients for the four parameters. However, this characteristic drove the GWNBRg model closer to the global model, which could not elaborate the spatial heterogeneity of the parameters. The optimum bandwidth of the GWNBR model was moderate and therefore showed a more explainable parameter distribution map than the other two GWR models.

4.3.4 Local analysis of GWR results

The differences between the coefficient distributions in northern and southern Indiana made it necessary to analyze local examples to determine possible factors that caused the heterogeneity. As described in the introduction, there were many unobserved factors (e.g., driver behavior, climate, and landcover). This thesis found that the landcover pattern coincided with the coefficient distribution of the pavement friction and curve length, which was illustrated by two typical regions of Indiana with different land covers and topographies. For example, southern Indiana has an area of forest while northern Indiana has cultivated crops, but there are some coefficient distribution patterns that matched the landcovers in Figure 4.4(a) and Figure 4.5(a). The southern Indiana forest region had higher absolute values for the AADT coefficients and low absolute values for the curve length and pavement friction coefficients, which reflects the relatively strong influence of traffic volume on the curve crash frequency in the forest curve segments. In northern Indiana, with its homogenous landcover, the parameters varied over space; and when compared with the southern Indiana forest area, the coefficients of AADT and the coefficients of pavement friction in areas

with significant coefficients were significantly lower at a 95% confidence level. The absolute value of the pavement friction coefficient in the forest area was about 75% less than that of the northern plain area. However, the landcover could not serve as a variable in the models as all of the curve segments were located in developed open space without varying landcover distributed around them.

In respect to curve distribution density, there also were patterns observed that can be seen in Figure 4.5. For the area with a significant coefficient in Figure 4.5(c), the locations with sparse curve segment distribution showed higher absolute values of the pavement friction coefficient than the remaining area at a 95% confidence level. Considering that the population density is low where there are cultivated crop landcovers and the highways are mostly straight explained why the pavement friction highly influenced the curve crash frequency.

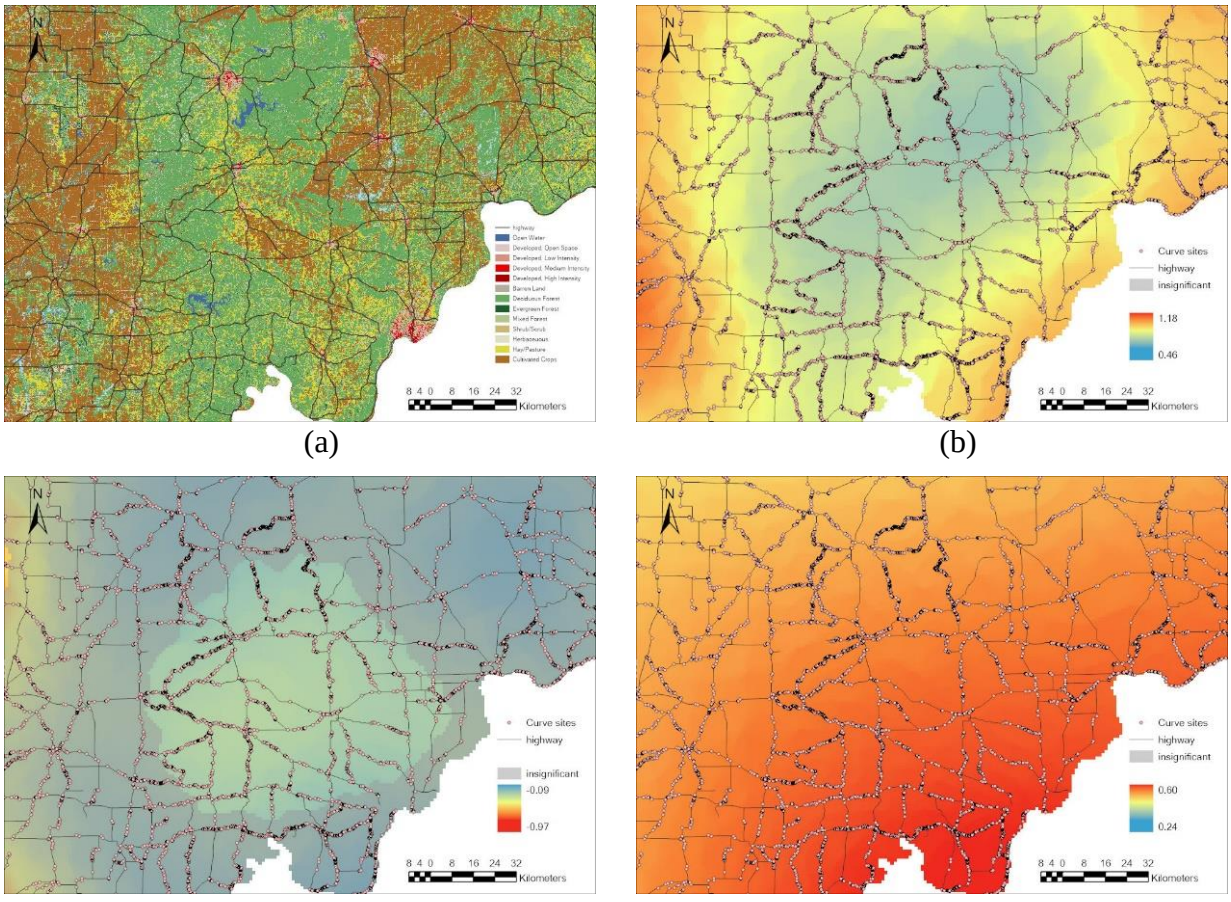

(a) (b)

(c) (d)

Figure 4.4. Landcover (a), distribution of (b) LOGL, (c) LOGF, and (d) LOGA in GWNBR in a forest area in southern Indiana.

Based on the three years of curve crash records for Indiana, this thesis concluded that the crash frequency during that time depended less on friction and curve length but rather was influenced by the AADT in the southern forest area. The remainder of Indiana, with mostly a cultivated crop landcover still had some other unobserved factors, such as curve density, which may have affected the curve crash frequency. This thesis concluded that the installation of HFST for curve segments on highways in the Indiana plain area would improve safety.

Generally, highway planners can directly use the results obtained from the spatial distribution analysis of the GWNBR model's coefficients in this thesis to develop security enhancement strategies in curve design and evaluate and prioritize these strategies from the perspective of security effects.

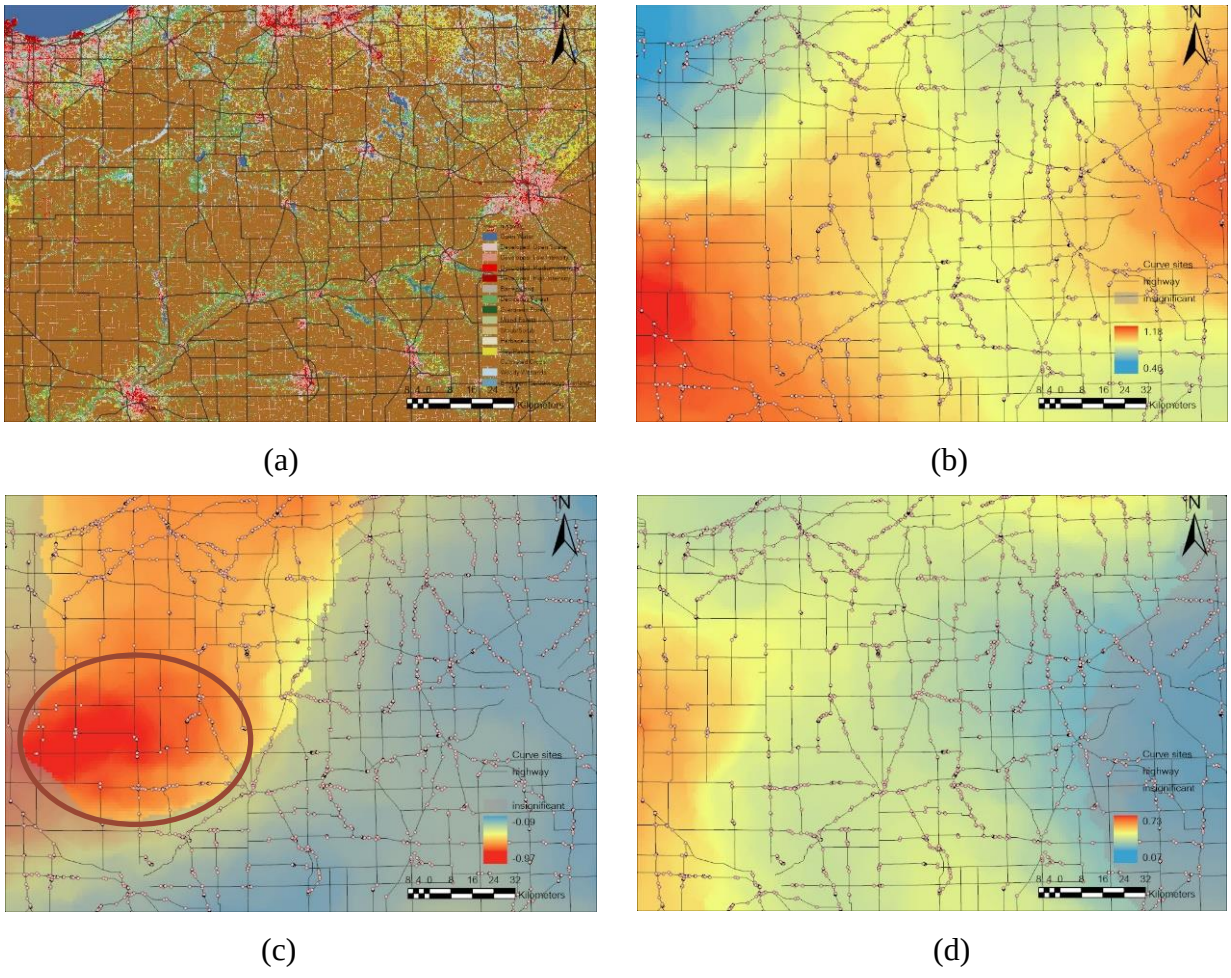

(a) (b)

(c) (d)

Figure 4.5. Landcover (a), distribution of (b) LOGL, (c) LOGF, and (d) LOGA in GWNBR in a plain area in northern Indiana.

4.4 Discussion

The estimated models in this thesis to determine the crash frequency occurring on the curves used the following explanatory variables: curve radius, curve length, pavement friction, and traffic volume, which were aggregated in individual curve segments. The GWPR model yielded the lowest MAD and the smallest absolute value of Moran's I by overfitting to the extreme values with its coefficient heterogeneity while the GWNBR model outperformed the others in terms of log likelihood and AICc. Since neither model proved non-autocorrelation of residual spatial distribution, the GWNBR model was the best approach that was able to capture the spatial heterogeneity between the frequency of curve crashes and the explanatory variables. Although the RPNB model incorporated unobserved heterogeneity in the modeling process and has been widely employed, it failed to account for the spatial correlation that existed across adjacent observations, which may result in biased parameter estimates and incorrect inference. The calibration process of the GWR approach is based on the First Law of Geography, which was implemented as all the attribute values over the area of interest were correlated, however, the near values were more related than the distant values. The GWPR model minimized MAD using a heterogeneous coefficient distribution pattern but had a significant number of incorrect signs for radius and friction, which may cause overfitting issues. The GWNBR model performed better than the GWNBRg model with a global dispersion parameter; and it was selected as the best local model depicting the non-stationary curve crash frequency coefficients statewide. In the local analysis of the GWNBR model variables distribution, the southern Indiana forest area’s pavement friction and curve length played a less critical role in reducing crash occurrence than other landcover regions, and the AADT was more crucial in that area. In the Indiana plain areas, the parameters also varied over space without considering other unobserved factors such as weather and driver behavior.

Other than spatial analysis, comparing the models’ CMF predictions and the observed CMF of HFST also played an important role. The average pavement friction of the 25 HFST installations across Indiana increased from 38.6 to 82.9. Substituting the pavement friction values before and after installing HFST into the models in this chapter yielded the predicted CMFs. The prediction results are presented in Table 4.6.

Table 4.6 HFST CMF predictions.

Source	CMF
Observation	0.701
ZINB (NB)	0.759
RPNB	0.752
GWPR	0.786
GWNBR	0.742
GWNBRg	0.751

Note that the prediction results for the ZINB and NB models were identical due to the insignificant friction parameter in the zero state of the ZINB model. Therefore, improving the friction only did not make a difference in the CMF calculation between them. The mean CMF prediction of these models ranged from 0.742 to 0.786, which all were higher than the CMF calculated from the observations. The best prediction in terms of the 25 HFST installations was provided by the GWNBR model, which further strengthened its dominant performance. However, the overall conservative results from these models also reflect the flaws of this series of models and database. Other possible reasons also could have originated from the HFST data collection, such as the small number of samples (25 sites) and the limited time period after their installation.

5. CONCLUSION

Traffic accident prevention and its spatial analysis have been receiving increased attention in recent years. This thesis comprehensively explored spatial modeling approaches along with the application of advanced non-spatial models to identify road curve crash frequency. The data used in this thesis included INDOT jurisdiction highway curve crash data as well as HFST installation information throughout the state.

The HFST safety performance evaluation of this thesis first identified 25 HFST sites installed between September and November of 2018, which then were digitized according to satellite images and their geometry features were extracted. As far as the crash analysis portion of this thesis, the locations of crashes that occurred between 2016 and 2019 were used to establish the crash frequencies for each HFST site in preparation for an EB before-after analysis. The estimated CMF of the Indiana HFST installations was found to be 0.701, which was close to the results of HFST-related research conducted by other states. But one year after-HFST crash count is not convincingly enough to draw solid conclusion about their safety performance. With more crash data available over a longer period of time after the HSFT installation, a practical application of this work is to do benefit/cost analysis on these HFST installations and offer suggestions for decision makers and practitioners from safety and economic perspectives.

This thesis mainly focused on modeling the curve crash frequency as the major reason for installing HFST is crash reduction. Crash frequency with spatial heterogeneity was employed to quantitively investigate its relationship with each curve segment's characteristics aggregated at both the macro and micro levels. Two types of models, i.e., non-spatial and spatial, were utilized to account for the spatial heterogeneity of the coefficients due to the unobserved factors over space. Poisson and GWPR models first were employed for the macro-level dataset. Then, for the micro-level dataset, the traditional NB model was specified as a basic global model to consider data over-dispersion, and a ZINB model was applied to solve the excessive zero observation problem. Both RPNB and GWR spatial approaches, including GWPR, GWNBR, and GWNBRg, were used to determine the preferable model for explaining road crash occurrence. The GWNBR model was promising for dispersed crash frequency data at the micro-level for safety planning compared to the other model in this thesis, especially for explaining the local coefficient distribution. In terms of spatial autocorrelation of the model's residuals, spatial models increased the p-value of Moran's

I in the macro-level and micro-level datasets, reflecting that it was able to sufficiently randomize the spatial distribution for the model residuals. The CMF predictions from all the micro-level models were relatively close to the EB analysis results, but all of them underestimated the safety performance of HFST, which will require additional crash data collection to verify.

The GWNBR model produced a moderate fluctuation of the curve segment's radius and the pavement friction's influence for crash frequency over space, suggesting a more realistic spatial-varying safety guidance value. These findings will help safety professionals achieve more accurate estimates of the safety of horizontal curves, allocate funds to reduce or prevent potential crashes, and design better road segments based on existing horizontal curve crash data to minimize crash risk. For example, HFST is suggested by this thesis for implementation on highway curves in the plain regions. In the hilly areas, some countermeasures such as limiting the traffic volume during peak hours, should be considered while implementing HFST if the terrain does not allow curve flattening. Note also that the calibration of this model needs to be designed again for regional crash modeling in another geographical area since the set of local parameters are not interchangeable over other spaces.

This work has some limitations. Since Indiana is dominated by cultivated crops and forests, it is difficult to reliably infer the effects of parameters in other less represented land covers. Furthermore, speed limit data are an important factor for a curve safety study. Although a non-stationary model could compensate for unavailable variables, adding speed limit data would possibly lead to more realistic modeling. Last but not least, our findings on both HFST safety performance and statewide crash modeling may need further validation through additional data.

There are several areas recommended for future work. First of all, it is not always true that all parameters are spatial-varying when too many variables are involved. Hence, a semi-parametric model is recommended for setting those variables without strong spatial variation stationary to a simplified model. Furthermore, to account for the local effects in both space and time, the extension on the temporal dimension of the GWR approach, i.e., the GTWR model, could be the favorable model for traffic safety studies. In addition, as shown in Chapter 4, a ZINB model proved to be an effective way to solve the excessive zero count in the micro-level dataset used by this thesis. Combined with a RPNB model and a GWNBR model, a zero-inflated random parameter negative binomial (ZIRPNB) model and a zero-inflated geographically weighted negative

binomial regression (ZIGWNBR) model could be beneficial for conducting spatial analysis of traffic crash modeling.

REFERENCES

Abdel-Aty, M., Lee, J., Siddiqui, C., & Choi, K. (2013). Geographical unit based analysis in the context of transportation safety planning. *Transportation Research Part A: Policy and Practice, 49*, 62-75.

Agresti, A. (2015). *Foundations of linear and generalized linear models*. John Wiley & Sons.

Aguero-Valverde, J., & Jovanis, P. P. (2006). Spatial analysis of fatal and injury crashes in Pennsylvania. *Accident Analysis & Prevention*, *38*(3), 618-625.

Albin, R. B., Brinkly, V., Cheung, J., Julian, F., Satterfield, C., Stein, W. J., ... & Hanscom, F. R. (2016). *Low-Cost Treatments for Horizontal Curve Safety 2016*, FHWA-SA-15-084, U.S. Federal Highway Administration Office of Safety.

Amoh-Gyimah, R., Saberi, M., & Sarvi, M. (2016). Macroscopic modeling of pedestrian and bicycle crashes: A cross-comparison of estimation methods. *Accident Analysis & Prevention*, *93*, 147-159.

Amoh-Gyimah, R., Saberi, M., & Sarvi, M. (2017). The effect of variations in spatial units on unobserved heterogeneity in macroscopic crash models. *Analytic Methods in Accident Research, 13*, 28-51.

Anastasopoulos, P. C., & Mannering, F. L. (2011). An empirical assessment of fixed and random parameter logit models using crash and non-crash-specific injury data. *Accident Analysis & Prevention, 43*(3), 1140-1147.

Bíl, M., Andrášik, R., Sedoník, J., & Cícha, V. (2018). ROCA–An ArcGIS toolbox for road alignment identification and horizontal curve radii computation. *PLoS One*, *13*(12), e0208407.

Buddhavarapu, P., Banerjee, A., & Prozzi, J. A. (2013). Influence of pavement condition on horizontal curve safety. *Accident Analysis & Prevention*, *52*, 9-18.

Cai, Q., Abdel-Aty, M., Lee, J., & Huang, H. (2019). Integrating macro-and micro-level safety analyses: a Bayesian approach incorporating spatial interaction. *Transportmetrica A: Transport Science*, *15*(2), 285-306.

Chen, E., & Tarko, A. P. (2014). Modeling safety of highway work zones with random parameters and random effects models. *Analytic Methods in Accident Research*, *1*, 86-95.

Chen, S., Saeed, T. U., Alqadhi, S. D., & Labi, S. (2019). Safety impacts of pavement surface roughness at two-lane and multi-lane highways: accounting for heterogeneity and seemingly unrelated correlation across crash severities. *Transportmetrica A: Transport Science*, *15*(1), 18-33.

da Silva, A. R. & Rodrigues, T. C. V. (2014). Geographically weighted negative binomial regression - incorporating overdispersion. *Statistics and Computing*, *24*(5), 769-783.

Dong, C., Richards, S. H., Clarke, D. B., Zhou, X., & Ma, Z. (2014). Examining signalized intersection crash frequency using multivariate zero-inflated Poisson regression. *Safety Science, 70*, 63-69.

Duddu, V. R. & Pulugurtha, S. S. (2012). Neural networks to estimate crashes at zonal level for transportation planning. In *European Transport Conference 2012Association for European Transport (AET) Transportation Research Board*.

El-Basyouny, K. & Sayed, T. (2009). Urban arterial accident prediction models with spatial effects. *Transportation Research Record, 2102*(1), 27-33.

FHWA 2019. Horizontal Curve Safety. https://safety.fhwa.dot.gov/roadway_dept/countermeasures/horicurves/. [Access Date: 11/24/2020].

Fotheringham, A. S., Brunsdon, C., & Charlton, M. (2003). *Geographically weighted regression: the analysis of spatially varying relationships*. John Wiley & Sons.

Fotheringham, A. S., Crespo, R., & Yao, J. (2015). Geographical and temporal weighted regression (GTWR). *Geographical Analysis, 47*(4), 431-452.

Fotheringham, A. S., & Oshan, T. M. (2016). Geographically weighted regression and multicollinearity: dispelling the myth. *Journal of Geographical Systems, 18*(4), 303-329.

Gooch, J. P., Gayah, V. V., & Donnell, E. T. (2016). Quantifying the safety effects of horizontal curves on two-way, two-lane rural roads. *Accident Analysis & Prevention, 92*, 71-81.

Gomes, M. J. T. L., Cunto, F., & da Silva, A. R. (2017). Geographically weighted negative binomial regression applied to zonal level safety performance models. *Accident Analysis & Prevention, 106*, 254-261.

Hauer, E. (1997). *Observational Before/after Studies in road safety. estimating the Effect of Highway and traffic engineering measures on road safety*. Pergamon press.

Hadayeghi, A., Shalaby, A. S., & Persaud, B. (2003). Macrolevel accident prediction models for evaluating safety of urban transportation systems. *Transportation Research Record, 1840*(1), 87-95.

Hadayeghi, A., Shalaby, A. S., & Persaud, B. N. (2010). Development of planning level transportation safety tools using Geographically Weighted Poisson Regression. *Accident Analysis & Prevention, 42*(2), 676-688.

Heiberger, R. M., Heiberger, R. M., & Burt Holland, B. H. (2015). *Statistical Analysis and Data Display an Intermediate Course with Examples in R*. Springer.

Himes, S., Porter, R. J., Hamilton, I., & Donnell, E. (2019). Safety evaluation of geometric design criteria: Horizontal curve radius and side friction demand on rural, two-lane highways. *Transportation Research Record, 2673*(3), 516-525.

Huang, H., Abdel-Aty, M. A., & Darwiche, A. L. (2010). County-level crash risk analysis in Florida: Bayesian spatial modeling. *Transportation Research Record*, *2148*(1), 27-37.

Imprialou, M., & Quddus, M. (2019). Crash data quality for road safety research: current state and future directions. *Accident Analysis & Prevention*, *130*, 84-90.

Geedipally, S. R., Pratt, M. P., & Lord, D. (2019). Effects of geometry and pavement friction on horizontal curve crash frequency. *Journal of Transportation Safety & Security*, *11*(2), 167-188.

Kim, D. H., Ramjan, L. M., & Mak, K. K. (2016). Prediction of vehicle crashes by drivers' characteristics and past traffic violations in Korea using a zero-inflated negative binomial model. *Traffic Injury Prevention*, *17*(1), 86-90.

Lee, J., Abdel-Aty, M., & Jiang, X. (2014). Development of zone system for macro-level traffic safety analysis. *Journal of Transport Geography*, *38*, 13-21.

Liu, C., Zhao, M., Li, W., & Sharma, A. (2018). Multivariate random parameters zero-inflated negative binomial regression for analyzing urban midblock crashes. *Analytic Methods in Accident Research*, *17*, 32-46.

Lyon, C., Persaud, B., Merritt, D., & Cheung, J. (2020). Empirical Bayes before-after study to develop crash modification factors and functions for high friction surface treatments on curves and ramps. *Transportation Research Record*, 0361198120957327.

Mannering, F. L., & Bhat, C. R. (2014). Analytic methods in accident research: Methodological frontier and future directions. *Analytic Methods in Accident Research*, *1*, 1-22.

Mannering, F. L., Shankar, V., & Bhat, C. R. (2016). Unobserved heterogeneity and the statistical analysis of highway accident data. *Analytic Methods in Accident Research*, *11*, 1-16.

Manual, H. S. (2010). Aashto. *Washington, DC*, *529*.

Merritt, D. K., Lyon, C., & Persaud, B. (2015). *Evaluation of Pavement Safety Performance*, FHWA-HRT-14-065. U.S. Federal Highway Administration.

Miaou, S. P. (1994). The relationship between truck accidents and geometric design of road sections: Poisson versus negative binomial regressions. *Accident Analysis & Prevention*, *26*(4), 471-482.

Moran, P. A. (1950). Notes on continuous stochastic phenomena. *Biometrika*, *37*(1/2), 17-23.

Musey, K., & Park, S. (2016). Pavement skid number and horizontal curve safety. *Procedia Engineering*, *145*, 828-835.

Musey, K. M. (2017). *Quantifying the Safety Impact of High Friction Surface Treatment Installations in Pennsylvania*. Villanova University.

Nakaya, T., Fotheringham, A. S., Brunsdon, C., & Charlton, M. (2005). Geographically weighted Poisson regression for disease association mapping. *Statistics in Medicine*, *24*(17), 2695-2717.

Nakaya, T., Fotheringham, S., Charlton, M., & Brunsdon, C. (2009). Semiparametric geographically weighted generalised linear modelling in GWR 4.0.

Peterson, R. (2016). California's Experience with HFST. Retrieved April 2021, from http://www.dot.ca.gov/hq/LocalPrograms/TCC/2016/March/California_Experience_with_HFST.pdf

Quddus, M. A. (2008). Modelling area-wide count outcomes with spatial correlation and heterogeneity: An analysis of London crash data. *Accident Analysis & Prevention*, *40*(4), 1486-1497.

Raihan, M. A., Alluri, P., Wu, W., & Gan, A. (2019). Estimation of bicycle crash modification factors (CMFs) on urban facilities using zero inflated negative binomial models. *Accident Analysis & Prevention*, *123*, 303-313.

Romero, M., Atisso, E. T., Wang, T., Slusher, L., & Tarko, A. (2017). Using GIS to determine locations for safety improvements. *Purdue GIS Day*

Saeed, T. U., Hall, T., Baroud, H., & Volovski, M. J. (2019). Analyzing road crash frequencies with uncorrelated and correlated random-parameters count models: An empirical assessment of multilane highways. *Analytic Methods in Accident Research*, *23*, 100101.

Schneider IV, W. H., Savolainen, P. T., & Moore, D. N. (2010). Effects of horizontal curvature on single-vehicle motorcycle crashes along rural two-lane highways. *Transportation Research Record*, *2194*(1), 91-98.

Shankar, V., Milton, J., & Mannering, F. (1997). Modeling accident frequencies as zero-altered probability processes: an empirical inquiry. *Accident Analysis & Prevention*, *29*(6), 829-837.

Shaon, M. R. R., Qin, X., Shirazi, M., Lord, D., & Geedipally, S. R. (2018). Developing a random parameters negative binomial-lindley model to analyze highly over-dispersed crash count data. *Analytic Methods in Accident Research*, *18*, 33-44.

Shaon, M. R. R., Schneider, R. J., Qin, X., He, Z., Sanatizadeh, A., & Flanagan, M. D. (2018). Exploration of pedestrian assertiveness and its association with driver yielding behavior at uncontrolled crosswalks. *Transportation Research Record*, *2672*(35), 69-78.

Silva, A. D., & Rodrigues, T. C. V. (2016). A SAS® macro for geographically weighted negative binomial regression. Data de acesso, 1(06), 2016.

Soroori, E., Mohammadzadeh Moghaddam, A., & Salehi, M. (2020). Modeling spatial nonstationary and overdispersed crash data: Development and comparative analysis of global and geographically weighted regression models applied to macrolevel injury crash data. *Journal of Transportation Safety & Security*, 1-25.

Srinivasan, R., Carter, D., & Bauer, K. M. (2013). *Safety performance function decision guide: SPF calibration vs SPF development*, FHWA-SA-14-004. U.S. Federal Highway Administration Office of Safety.

Venkataraman, N. S., Ulfarsson, G. F., Shankar, V., Oh, J., & Park, M. (2011). Model of relationship between interstate crash occurrence and geometrics: exploratory insights from random parameter negative binomial approach. *Transportation Research Record*, *2236*(1), 41-48.

Venkataraman, N., Ulfarsson, G. F., & Shankar, V. N. (2013). Random parameter models of interstate crash frequencies by severity, number of vehicles involved, collision and location type. *Accident Analysis & Prevention*, *59*, 309-318.

Venkataraman, N., Shankar, V., Ulfarsson, G. F., & Deptuch, D. (2014). A heterogeneity-in-means count model for evaluating the effects of interchange type on heterogeneous influences of interstate geometrics on crash frequencies. *Analytic Methods in Accident Research*, *2*, 12-20.

Von Quintus, H. L. & Mergenmeier, A. (2015). *Case study: Kentucky Transportation Cabinet's High Friction Surface Treatment and Field Installation Program*, FHWA-SA-15-038. U.S. Federal Highway Administration. Office of Safety.

Washington, S., Karlaftis, M. G., Mannering, F., & Anastasopoulos, P. (2020). *Statistical and Eeconometric Methods for Transportation Data Analysis*. CRC press.

Wan, D. (2018). *The Spatial Analysis of Crash Frequency and Injury Severities in New York City: Applications of Geographically Weighted Regression Method* (Doctoral Dissertation, The City College of New York).

Wang, C., Quddus, M., & Ison, S. (2009). The effects of area-wide road speed and curvature on traffic casualties in England. *Journal of Transport Geography*, *17*(5), 385-395.

Wilson, B. T., Brimley, B. K., Mills, J., Zhang, J., Mukhopadhyay, A., & Holzschuher, C. (2016). Benefit–cost analysis of Florida high-friction surface treatments. *Transportation Research Record*, *2550*(1), 54-62.

Xin, C., Wang, Z., Lin, P. S., Lee, C., & Guo, R. (2017). Safety effects of horizontal curve design on motorcycle crash frequency on rural, two-lane, undivided highways in Florida. *Transportation Research Record*, *2637*(1), 1-8.

Xin, C., Wang, Z., Lee, C., & Lin, P. S. (2017). Modeling safety effects of horizontal curve design on injury severity of single-motorcycle crashes with mixed-effects logistic model. *Transportation Research Record*, *2637*(1), 38-46.

Xu, P. & Huang, H. (2015). Modeling crash spatial heterogeneity: Random parameter versus geographically weighting. *Accident Analysis & Prevention*, *75*, 16-25.

Ziakopoulos, A., & Yannis, G. (2020). A review of spatial approaches in road safety. *Accident Analysis & Prevention*, *135*, 105323.